

Existence and Stability of Traveling Pulses in a Reaction-Diffusion-Mechanics System

Matt Holzer*, Arjen Doelman[†], Tasso J. Kaper[‡]

July 5, 2012

Abstract

In this article, we analyze traveling waves in a reaction-diffusion-mechanics (RDM) system. The system consists of a modified FitzHugh-Nagumo equation, also known as the Aliev-Panfilov model, coupled bidirectionally with an elasticity equation for a deformable medium. In one direction, contraction and expansion of the elastic medium decreases and increases, respectively, the ionic currents and also alters the diffusivity. In the other direction, the dynamics of the R-D components directly influence the deformation of the medium. We demonstrate the existence of traveling waves on the real line using geometric singular perturbation theory. We also establish the linear stability of these traveling waves using the theory of exponential dichotomies.

AMS(MOS) numbers: 35K57, 74H20, 35C07, 35P15

Keywords: traveling waves, reaction-diffusion-mechanics equations, waves in deformable media, geometric singular perturbation theory, spectral stability, exponential dichotomies

1 Introduction

Traveling waves in reaction-diffusion equations have been studied extensively in many areas of science and technology, see for example [22, 35, 36]. A prototypical example in neuroscience is the FitzHugh-Nagumo (FHN) equation, see [20]. This PDE models the transmembrane voltage for nerve cells and the dynamics of a recovery variable. Traveling waves in the FHN equation represent the propagation of action potentials along nerve cells. Fundamental characteristics of these traveling waves in FHN, such as their profiles, speeds, decay rates, and stability properties, are by now well understood. Initial studies employed piece-wise linear models, [26, 32]. Existence and stability for the full smooth FHN PDE was established in [4, 15, 17].

One of the interesting new directions in which the FitzHugh-Nagumo type modeling has been taken recently involves the bidirectional coupling of a reaction-diffusion equation and a mechanics equation that governs the deformations of the medium in which the action potential propagate. Such models are referred to as reaction-diffusion-mechanics (RDM) models. They are a natural next step for modeling wave propagation in certain deformable media using continuum models, and they present novel mathematical challenges.

A prototype example is the RDM model developed by Panfilov, Keldermann, and Nash [27, 30]. They modeled the mechanical deformation of a 2-D patch of heart muscle fiber using equations for elastic media. Then, they bidirectionally coupled this elasticity equation to a modified FitzHugh-Nagumo equation. In one direction, the stretching and contraction of the heart muscle directly change the magnitudes of the current and diffusivity in the voltage equation, because the deformation directly alters the number of ion channels that are open or closed. In the other direction, variations in the magnitude of the current result in changes in the deformation of the medium. This model was motivated by experiments, including those in [21, 24].

The coupled RDM system with two-dimensional elasticity equations involves a second-order PDE coupled to the reaction-diffusion equations. Hence, it is difficult to analyze directly. However, locally, the heart muscle

*School of Mathematics, University of Minnesota, 127 Vincent Hall, 206 Church St. SE, Minneapolis MN 55455, USA

[†]Mathematisch Instituut, Universiteit Leiden, Postbus 9512, 2300 RA Leiden, the Netherlands

[‡]Department of Mathematics and Statistics & Center for BioDynamics Boston University, 111 Cummington Street, Boston, MA 02215, USA

tissue consists, to a good approximation, of parallel muscle fibers. Therefore, the dominant deformations are one-dimensional, corresponding to the stretch and contraction of individual fibers. While this approximation neglects important effects created by the coupling between adjacent fibers, it will be useful as a first step in the analysis of the full two-dimensional model. In addition, the analysis of this one-dimensional model on the real line will be a building block for the treatment of the coupled RDM system on a periodic domain.

In this article, we study the following RDM model on the real line,

$$\begin{aligned} \frac{\partial u}{\partial t} &= \frac{1}{F} \frac{\partial}{\partial X} \left(\frac{1}{F} \frac{\partial u}{\partial X} \right) - ku(u-a)(u-1) - uw \\ \frac{\partial w}{\partial t} &= \epsilon(ku - w) \\ F(X, t) &= \frac{1}{2} + \frac{M}{4c_1} + \frac{1}{2} \sqrt{\left(1 + \frac{M}{2c_1}\right)^2 - \frac{2}{c_1} w(X, t)}. \end{aligned} \tag{1.1}$$

Here, the R-D components u and w are the same as in the modified FitzHugh-Nagumo equation studied in [30]. Namely, u represents voltage and w a recovery variable. The key parameters are a , which measures the degree of excitability in the medium and k , a rate constant. The coupling between u and w is nonlinear, exactly as in the Aliev-Panfilov modification of the classical FHN equation, see [1], and this contrasts with the linear coupling in the classical FHN equation. In addition, the separation of time scales between the u and w dynamics is modeled by the asymptotically small parameter ϵ . See Section 2.1.

The mechanical component, modeled by the deformation $F(X, t)$, is derived from the equation for an elastic medium using a Piola-Kirchhoff type stress tensor under the assumption that the medium is hyperelastic. It is assumed that the stress is a linear combination of active and passive components and that the active stress is dependent only on the recovery variable w . The parameter c_1 is a measure of the internal energy of the deformable medium and it scales the relative importance of the passive and active stresses. The medium is assumed to be in mechanical equilibrium, which for one-dimensional objects is equivalent to constant stress throughout. The constant M is this stress, measured in material coordinates. Application of these conditions simplifies the 1-D elastic medium equations to a single formula for the deformation F , as in (1.1). See Section 2.2.

In system (1.1), the bidirectional coupling between the R-D components u and w and mechanical component F is modeled by the w dependence in the formula for the deformation F and the dependence of the diffusivity in the voltage equation on the deformation F . In addition, it is possible to incorporate a stretch activated current, I_{SAC} into (1.1). However, the incorporation of stretch activated currents is more applicable to bounded domains (for reasons that will be explained in section 2.4) so we will focus on the case $I_{SAC} = 0$.

The first main result of this article is the existence of traveling waves in the RDM system (1.1) on the real line. See Theorem 1 in Section 3 below. These traveling waves are similar to the fast pulses of the classical FitzHugh-Nagumo equation, consisting of fronts and backs concatenated together, interspersed with quiescent and active phases. We focus here on the regime in which the back jumps from the knee of the active branch, rather than from below the knee, where the knee is the nonhyperbolic local maximum of the right (active) branch of the cubic nullcline in (1.1). Pulses of this type are relevant for cardiac models and also present mathematical challenges due to the non-hyperbolicity of the knee. The existence analysis consists of constructing the appropriate singular homoclinic solution and showing that it lies in the transverse intersection of the appropriate center-unstable and center-stable manifolds of the asymptotic state. Center manifold theory and geometric desingularization near the knee are also needed to carry out this construction. This aspect of the work is similar to the approach developed recently in [3].

The second main result is the spectral stability analysis of the traveling waves in the RDM model (1.1). We determine the parameter regime in which the traveling waves are stable using the method of exponential dichotomies. See Theorem 3 and its proof in Section 4–6. Exponential dichotomies are shown to exist over the individual segments of the singular homoclinic solution. The stable and unstable subspaces are tracked over the entire pulse using the estimates from these dichotomies along each segment, and roughness of the dichotomies is used to bootstrap up to the full system with $0 < \epsilon \ll 1$. We note that this approach differs fundamentally from that used in [17] for the classical FHN equation and from that used in [3] for a cardiac model. Exponential dichotomies have been used to establish spectral stability in other partial differential

equations, see for example, Section 3.2 in [34]. We remark that the results about the spectrum of the linearized operator in this article can also be used to obtain semi-group results, especially concerning the spectrum of the operator obtained by exponentiating this linear operator. We refer the reader to [2], as well as to the more recent analysis in [14, 33], for general results.

Besides being of interest in their own rights for the RDM model (1.1), the existence and stability analyses we present are essential building blocks for other RDM modeling in this direction. The RDM model developed in Section 2 also applies to 1-D models on finite domains and on periodic domains. The existence analysis and the stability analysis (via exponential dichotomies) are well-suited for spatially-periodic problems. In addition, we hope that the methods developed here may find application in other RDM systems. One such system involves mechanically induced oscillations in a gel [39]. In addition, there are a number of phenomena associated to pulse propagation, such as blocking and propagation failure, and it would be of interest to study them also in this RDM system.

The article is organized as follows. In section 2, the RDM model of Panfilov, Keldermann and Nash is developed in one dimension. In section 3, we establish the existence of a traveling pulse. Then in sections 4-6 the spectral stability of this pulse is established.

2 Derivation of the RDM Model

In this section, we build up the reaction-diffusion-mechanics (RDM) model in one dimension. We follow very closely the work of Panfilov, Keldermann, and Nash [30] who developed the model in higher dimensions.

2.1 Equations for electrical activity

We consider a modified Fitz-Hugh Nagumo model in one spatial dimension. Introduced in [1], this modified Fitz-Hugh Nagumo equation models the excitation and propagation of electric currents in cardiac tissue. The two state variables are u , which represents the transmembrane potential and w , a recovery variable. They are governed by the following reaction-diffusion equations:

$$\begin{aligned} u_t &= Du_{xx} - f(u, w) \\ w_t &= \epsilon(u)(ku - w), \end{aligned} \tag{2.1}$$

with $f(u, w) = ku(u - a)(u - 1) + uw$, where D , k and a are parameters, and $\epsilon(u)$ is a step function with $\epsilon(u) = 1$ if $u < .05$ and $\epsilon(u) = .1$ otherwise. This step function is included to capture the time scale of recovery. The domain can be taken to be the finite interval $[0, L]$, a ring or the infinite real line \mathbb{R} .

2.2 Mechanical Deformation

In cardiac cells, changes in transmembrane potential lead to contraction of the cardiac tissue. Following [27, 30], we use finite deformation elasticity theory to develop a mechanical model of deformation to couple to the excitable model given by (2.1). For a reference on finite deformation elasticity, see [25, 16] among others. In one dimension many things simplify. In particular, all quantities are scalar functions instead of tensors. Our approach is to consider the one dimensional medium as being embedded in a three dimensional medium, but require the medium to be undeformable in all directions other than the embedded one.

We begin with a set of reference (material) coordinates, X , which at some time t have deformed to a new position given by

$$x = \phi(X, t).$$

The deformation of the material at time t is represented by $F = \frac{\partial x}{\partial X}$. In deformed coordinates, the stress, or force per unit area, at a point x is given by $\tilde{T}(x)$. It is preferable to work in terms of material coordinates, so we define a second stress tensor, $T(X)$, that measures the stress in terms of force per unit undeformed area. This tensor is known as the second Piola-Kirchhoff stress tensor and is related to \tilde{T} by $FT = \tilde{T}$. For any arbitrary deformation, conservation of momentum implies that the tissue is in equilibrium if

$$\frac{\partial}{\partial X} FT = 0. \tag{2.2}$$

In deformed coordinates, the equilibrium condition is given by $\frac{\partial \tilde{T}}{\partial x} = 0$. Postulating an internal energy of the form $W(F) = c_1(F - 1)^2$, we may derive via conservation of energy that the stress is given by

$$T(X, t) = \frac{1}{F} \frac{\partial W}{\partial F} = 2c_1 \frac{F - 1}{F}. \quad (2.3)$$

This is known as the passive stress. Combining the conditions (2.2) and (2.3), we arrive at the governing equation for the deformation in the absence of electrical coupling,

$$\frac{\partial F}{\partial X} = 0.$$

To couple the deformation to the potential u , we follow [27, 30] and introduce an active stress, $T_a(X, t)$, which evolves in time according to

$$\frac{\partial T_a}{\partial t} = \epsilon(u)(k_T u - T_a),$$

where k_T is a parameter. The active stress sums with the passive stress (2.3) to yield the total stress,

$$T(X, t) = 2c_1 \frac{F - 1}{F} + \frac{T_a}{F^2}.$$

The equilibrium condition (2.2) is used to derive an expression for the evolution of the deformation $F(X, t)$. In particular, we have that

$$\frac{\partial}{\partial X} \left(2c_1(F - 1) + \frac{T_a}{F} \right) = 0.$$

One way in which to interpret this condition is that the product of the deformation and the second Piola-Kirchhoff stress is equal to a constant in X . In other words, we have

$$2c_1(F - 1) + \frac{T_a}{F} = M,$$

for some M which can depend on t but not on X . We apply the equilibrium condition (2.2) and solve for the deformation as

$$F(X, t) = \frac{1}{2} + \frac{M}{4c_1} + \frac{1}{2} \sqrt{\left(1 + \frac{M}{2c_1}\right)^2 - \frac{2}{c_1} T_a(X, t)}. \quad (2.4)$$

This formula for the deformation F is almost the final form that is stated in the RDM model (1.1).

Remark 1. Note that if $T_a > \frac{c_1}{2} \left(1 + \frac{M}{2c_1}\right)^2$, the mechanical model no longer possesses static equilibrium and (2.4) is no longer valid. To extend the model to the regime of large T_a , a PDE for the temporal evolution of the displacement would have to be included representing the conservation of momentum. Since we are interested in traveling pulses with at most small perturbations, in this article we will focus on the case when the mechanical model is in equilibrium and the deformation can be expressed explicitly as in (2.4).

Remark 2. The spatial constant M is related to the boundary conditions placed upon the mechanical medium. Natural boundary conditions for mechanical models involve geometric constraints, surface tractions or some combination of the two. Thus, they are conditions placed upon either the displacement ϕ or the stress \tilde{T} . In one spatial dimension, a common mechanical boundary condition to impose is zero total displacement. Integrating (2.4) gives an expression for the displacement

$$\phi(X, t) = \left(\frac{1}{2} + \frac{M}{4c_1} \right) X + \frac{1}{2} \int_0^X \sqrt{\left(1 + \frac{M}{2c_1}\right)^2 - \frac{2}{c_1} T_a(\sigma, t)} d\sigma,$$

where we have chosen to fix the left boundary at $X = 0$. The right boundary is fixed in space with the following implicit choice of M (suppose that the domain is the unit interval $[0, L]$),

$$\left(1 - \frac{M}{2c_1}\right)L - \int_0^L \sqrt{\left(1 + \frac{M}{2c_1}\right)^2 - \frac{2}{c_1} T_a(\sigma, t)} d\sigma = 0.$$

Finally, with the solution M in hand, then the value that F must attain at the right boundary can be easily obtained using (2.4).

Remark 3. *When the domain is infinite, the constant $\frac{M}{2c_1} + 1$ will be taken to be the imposed deformation at $X = \pm\infty$. A natural choice for M would be zero implying zero deformation at infinity. We will opt to leave M as a parameter so that this work more easily generalizes to the periodic case, where values of $M \neq 0$ are physical.*

2.3 Influence of deformation on diffusivity

The deformation is coupled back to the original equation by altering the diffusion rates of the u variable. Thus, the Laplacian operator in (2.1) transforms to

$$\frac{\partial^2}{\partial x^2} = \frac{1}{F} \frac{\partial}{\partial X} \left(\frac{1}{F} \frac{\partial}{\partial X} \right). \quad (2.5)$$

2.4 Stretch activated current and bounded versus unbounded domains

The deformation is also coupled to the voltage equation via the stretch activated current. If the medium is contracting ($F < 1$), then the current is turned off; otherwise, when the medium is stretched ($F > 1$) the current is on. The current is,

$$I_{SAC} = G_s \chi(F) (F - 1) (u - E_s), \quad (2.6)$$

where G_s and E_s represent the maximal conductance and the reversal potential of this current and $\chi(F)$ is a smooth cutoff function which is identically one for $F > 1$ and identically zero for all $F < b < 1$ (see [30]).

The stretch activated current plays a significant dynamic role in problems on bounded domains. See for example [30], where pacemaking behavior was observed as a result of the stretch activated current. Bounded domains can give rise to stretch in a dynamic way, see for example Remark 2. Consider zero displacement boundary conditions. If the medium is locally excited at some point this leads to contraction nearby. Total zero displacement then requires that some other part of the domain must be stretched (i.e. $M(t)$ increases). This can lead to the local destabilization of the background state. Coupled with the stable propagation of pulses, this can give rise to recurrent oscillatory behavior of the form observed in [30].

To see why it plays a less essential role on unbounded domains we recall the functional form of the deformation. The domain is stretched when $F > 1$. For unbounded problems where M is a parameter then stretching can only occur in one of two ways: when M is positive or when w is sufficiently negative. However, since u is always positive we see that negative w is unphysical. This leaves only the dependence on M , which gives the induced stretch at equilibrium. This dependence can do one of two things. Either it leaves the background state stable, in which case the problem is qualitatively similar, or it can destabilize the background state leading to significant changes in the behavior.

While we consider only the case of $I_{SAC} = 0$, we note that for G_s sufficiently small the inclusion of the stretch activated current only shifts the nullclines of the problem. As a result, the same analysis could be applied to that case and a homoclinic orbit could be obtained representing a pulse connecting the stable fixed point near the origin to itself. Since the inclusion of weak stretch activated currents does not change the dynamics, but introduces more complicated expressions we will consider only the simpler case $I_{SAC} = 0$. As we noted above, larger values of G_s will lead to the destabilization of the fixed point so that it is of no physical interest to consider a traveling pulse homoclinic to that point.

2.5 Full model and parameters

The full model is obtained by incorporating the stretch activated current (2.6) and diffusive effects (2.5) into the electrical model (2.1). The result is

$$\begin{aligned}\frac{\partial u}{\partial t} &= \frac{D}{F} \frac{\partial}{\partial X} \left(\frac{1}{F} \frac{\partial u}{\partial X} \right) - ku(u-a)(u-1) - uw - I_{SAC} \\ \frac{\partial w}{\partial t} &= \epsilon(u)(ku - w) \\ \frac{\partial T_a}{\partial t} &= \epsilon(u)(k_T u - T_a) \\ F(X, t) &= \frac{1}{2} + \frac{M}{4c_1} + \frac{1}{2} \sqrt{\left(1 + \frac{M}{2c_1}\right)^2 - \frac{2}{c_1} T_a(X, t)}.\end{aligned}$$

We will make several simplifications of this model in order to facilitate the forthcoming analysis. First, we note that the equations for the active stress and the slow variable w are similar, so we elect to study the case when $T_a = w$ (i.e. $k_T = k$). Second, the step function $\epsilon(u)$ introduces non-trivial difficulties in applying the tools of geometric singular perturbation theory. For that reason, we will study the case when $\epsilon(u) = \epsilon$. We could alternatively study the case when $\epsilon(u)$ is an asymptotically small step function, smoothed in an appropriate manner. In the future, we would like to extend the analysis that follows to the case of u dependent ϵ , but we will not focus on that case here. In addition, we will first study the case of $I_{SAC} = 0$, as we described above. Finally, since we consider this model on all of \mathbb{R} we set $D = 1$ by a rescaling of the spatial variable.

With these simplifications, the resulting model is precisely (1.1) and this is the model we will study in this paper.

Remark 4. *From this point forward we will refer to the deformation as a function of the recovery variable alone. This is because with M fixed, the only spatial and temporal dependence of F is through the recovery variable w .*

3 Existence Analysis

In this section, we will establish the existence of traveling waves for the RDM model, (1.1). Such structures arise as time-independent, homoclinic orbits in an appropriate traveling reference frame. We introduce a coordinate $\xi = X + ct$ for $c > 0$ and express the partial differential equation in these coordinates as,

$$\begin{aligned}u_t &= \left(\frac{1}{F}\right) \frac{\partial}{\partial \xi} \left(\frac{1}{F} \frac{\partial u}{\partial \xi}\right) - cu_\xi - ku(u-a)(u-1) - uw \\ w_t &= -cw_\xi + \epsilon(ku - w),\end{aligned}\tag{3.1}$$

with $F(w)$ given as in (1.1). Time independent solutions of these equations satisfy the ordinary differential equations,

$$\begin{aligned}\left(\frac{1}{F}\right) \frac{\partial}{\partial \xi} \left(\frac{1}{F} \frac{\partial u}{\partial \xi}\right) - cu_\xi - ku(u-a)(u-1) - uw &= 0 \\ w_\xi &= \frac{\epsilon}{c}(ku - w).\end{aligned}\tag{3.2}$$

We convert these equations into a system of first order equations,

$$\begin{aligned}u' &= F(w)v \\ v' &= cF^2(w)v + kF(w)u(u-a)(u-1) + F(w)uw \\ w' &= \frac{\epsilon}{c}(ku - w).\end{aligned}\tag{3.3}$$

This system has a unique rest point at $(u, v, w) = (0, 0, 0)$. We will exploit the singularly perturbed nature of these equations to construct singular solutions. Then, we will show that there is a true traveling

wave solution of (3.2) that shadows the singular solution for asymptotically small values of ϵ . The proofs will be geometric in nature. We will focus on the center-unstable manifold of the rest point at $(0, 0, 0)$. Also we will study the dynamics near the fold point on the right, active branch in system (3.3). The fold point is a non-hyperbolic rest point of the fast system associated to (3.3), and the analysis can be carried out using the method of geometric desingularization, see [8, 23] for example.

For the purposes of this paper, we will often illustrate our results in the case of $k = 8$, $a = .05$ and $c_1 = 10$, which are similar to the values used in [30]. However, the proof holds for much more general parameter values, which we will now define.

Definition 1. *The set, labelled Π , of allowable parameters (k, a, c_1, M) for the model in (1.1) consists of those parameters that satisfy:*

1. $a \in (0, 1/2)$ and $k > 0$,
2. The deformation is always real and positive, i.e. $\frac{k}{2c_1}(1-a)^2 < (1 + \frac{M}{2c_1})^2$, recall (2.4) and that T_a has been replaced by w ,
3. The parameters satisfy,

$$\sqrt{2k} \left(\frac{1}{F(0)} \left(\frac{1}{2} - a \right) - \frac{1}{F(\frac{k}{4}(1-a)^2)} \frac{(1+a)}{4} \right) > 0, \quad (3.4)$$

Note that the set of parameters studied in [30], $(k, a, c_1, M) = (8, .05, 10, 1)$, lies in Π . Condition 3 in Definition 1 may be interpreted geometrically as requiring that the wavespeed selected by the front (see (3.8)) is strictly greater than the wave speed selected by the back (see (3.10)). Hence, the jump back must occur along the center direction at the knee, see Figure 2.

For $(k, a, c_1, M) \in \Pi$, we will show that the model gives rise to traveling waves in the form of a homoclinic orbit connecting the rest point at $(0, 0, 0)$ to itself. Our approach will be a geometric one, following the work of [17], where existence and stability of traveling wave orbits in the Fitz-Hugh Nagumo equation are studied. The primary complication in our case is that the homoclinic connection will pass close by the non-hyperbolic point on the right slow manifold. Therefore, the techniques in [17] will need to be adapted to this case. A similar construction has already been performed in [3] for a different two component cardiac model in which the homoclinic connection passes near a non-hyperbolic point. We will establish the following result.

Theorem 1. *Suppose that $(k, a, c_1, M) \in \Pi$. Then there exists $\epsilon_1 > 0$ such that for all $0 < \epsilon < \epsilon_1$, there exists $c(\epsilon) = c(0) + \mathcal{O}(\epsilon)$ with $c(0) = \frac{\sqrt{2k}}{F(0)} (\frac{1}{2} - a)$ for which the problem (1.1) has a traveling wave solution of the form $(U(X + ct), W(X + ct))$ with $\lim_{\xi \rightarrow \pm\infty} (U, W) = (0, 0)$.*

This theorem is proven in two steps. First, a singular traveling wave solution is constructed for $\epsilon = 0$, see Section 3.1. Then, it is shown that this singular solution persists for small, positive values of ϵ , see Section 3.2, completing the proof of the theorem. Further information about the decomposition of the wave is given in Section 3.3, which will be useful for the stability analysis presented in the later sections.

3.1 The singular solution

3.1.1 The slow and fast subsystems

The system in (3.3) is a singularly perturbed equation possessing a cubic slow manifold consisting of two stable branches and one unstable branch. The slow subsystem can be found by a rescaling of the independent variable, $z = \epsilon\xi$, and then setting $\epsilon = 0$,

$$\begin{aligned} 0 &= F(w)v \\ 0 &= cF^2(w)v + kF(w)u(u-a)(u-1) + F(w)uw \\ \frac{dw}{dz} &= \frac{1}{c}(ku - w). \end{aligned}$$

Thus, since $F(w) > 0$ for all parameters in Π , the critical slow manifold is given by the set $\{v = 0\}$ and $\{u = 0\} \cup \{w = -k(u-a)(u-1)\}$.

Definition 2. The set $\mathcal{S}_L := \{v = 0, u = 0\}$ is the left critical slow manifold. Likewise, the set $\mathcal{S}_R := \{v = 0, w = -k(u - a)(u - 1), w > \frac{1+a}{2}\}$ is the right critical slow manifold.

On the other hand, setting $\epsilon = 0$ in (3.3) yields the fast subsystem. Here $w' = 0$ and therefore the recovery variable w and the deformation $F(w)$ act as parameters. The fast system has fixed points at $(u, v) = (0, 0), (U_1(w), 0), (U_2(w), 0)$, where

$$U_1(w) = \frac{1+a}{2} - \frac{1}{2}\sqrt{(1-a)^2 - \frac{4w}{k}},$$

and

$$U_2(w) = \frac{1+a}{2} + \frac{1}{2}\sqrt{(1-a)^2 - \frac{4w}{k}}.$$

3.1.2 The Front

For $w = 0$, we seek a leading order solution connecting the reduced fixed point on \mathcal{S}_L at $(u, v, w) = (0, 0, 0)$ to the fixed point on \mathcal{S}_R at $(u, v, w) = (U_2(0), 0, 0)$ for some value of the wave speed c . In order to describe the geometry most fully, it is convenient to work first with a general fixed value of w , which we label w_0 , and then to set $w_0 = 0$ to obtain the desired result.

For some fixed value of $w = w_0$, we seek a leading order solution connecting the reduced fixed point on \mathcal{S}_L at $(u, v, w) = (0, 0, w_0)$ to the fixed point on \mathcal{S}_R at $(u, v, w) = (U_2(w_0), 0, w_0)$ for some value of the wave speed c . The planar ($w = w_0$) problem is given by

$$\begin{aligned} u' &= Fv \\ v' &= cF^2v + kFu(u - U_1)(u - U_2). \end{aligned} \quad (3.5)$$

Dividing these equations we find

$$v \frac{dv}{du} = cFv + ku(u - U_1)(u - U_2). \quad (3.6)$$

To find the desired solution, we follow [5] and assume $v = \alpha u(u - U_2)$ for some value of α . With this assumption we can use (3.6) to compute

$$u(u - U_2) (\alpha^2 u + \alpha^2(u - U_2) - cF\alpha - k(u - U_1)) = 0.$$

We solve order by order in u to conclude

$$\begin{aligned} \alpha &= \pm\sqrt{\frac{k}{2}} \\ c &= \frac{k}{\alpha F} \left(U_1 - \frac{U_2}{2} \right). \end{aligned} \quad (3.7)$$

The requirement that $c > 0$ implies that α must share the sign of $U_1 - U_2/2$. A quick computation shows that the switch from negative to positive α occurs at,

$$w_{zero} = \frac{k}{4}(1-a)^2 - \frac{k}{36}(1+a)^2.$$

Then, for all $w_f < w_{zero}$, $\alpha = -\sqrt{k/2}$ and the leading order wave speed of the front is fixed to be

$$c(w_f) = \frac{\sqrt{2k}}{F} \left(\frac{U_2}{2} - U_1 \right).$$

In particular, for the case of the homoclinic pulse studied here, $w_f = 0$ and hence the speed of the front is

$$c(0) = \frac{\sqrt{2k}}{F(0)} \left(\frac{1}{2} - a \right). \quad (3.8)$$

With the wave speed fixed by (3.7), we may compute the leading order equation for the front by plugging the ansatz $v = \alpha u(u - U_2)$ into (3.5) and solving for $u(\xi)$,

$$u_f(\xi) = \frac{U_2 e^{\sqrt{\frac{k}{2}} F(w_f) U_2 \xi}}{1 + e^{\sqrt{\frac{k}{2}} F(w_f) U_2 \xi}}.$$

In the case of the pulse, $w_f = 0$ and we have,

$$u_f(\xi) = \frac{e^{\sqrt{\frac{k}{2}} F(0) \xi}}{1 + e^{\sqrt{\frac{k}{2}} F(0) \xi}}.$$

Fronts of the traveling waves are given to leading order by this formula.

3.1.3 The Back

The front selects the wavespeed of the pulse. In turn, the wavespeed of the pulse selects the particular value of w for which a jump back exists connecting the right slow manifold to the left slow manifold. As mentioned above, we will focus on the case when this jump occurs at the knee. The knee is given by the value of w for which $U_2(w) = U_1(w)$,

$$w_{knee} = \frac{k}{4}(1 - a)^2. \quad (3.9)$$

Proceeding as we did for the front, we find that there exists a critical wave speed (again $c > 0$),

$$c(w_{knee}) = c_{crit}, \quad \text{where} \quad c_{crit} = \frac{\sqrt{2k}}{4F(w_{knee})}(1 + a), \quad (3.10)$$

for which a connection of the form $v = \alpha u(u - U_2)$ exists between the knee at $((1 + a)/2, 0, k(1 - a)^2/4)$ and the left branch of the slow manifold at $(0, 0, k(1 - a)^2/4)$. This formula is computed analogously to the case of the front, except with $\alpha = \sqrt{k/2}$ so that the back departs from \mathcal{S}_R . In addition, by a trapping region argument and results of [5] we find that for all values of $c > c_{crit}$, a connection also exists between the knee and the left branch of the critical slow manifold. This solution will no longer satisfy a quadratic relationship between u and v . Instead, it departs the knee along the center-unstable direction and approaches the left branch tangent to the stable direction in the stable manifold of the left slow manifold.

When $c(w_f) > c_{crit}$ we will show that the reduced equation along the back has a solution with algebraic decay rate as $\xi \rightarrow -\infty$. Thus, we use (3.5) with $U_1 = U_2$,

$$\begin{aligned} u' &= Fv \\ v' &= cF^2v + kFu(u - U_2)^2. \end{aligned}$$

Linearizing at the knee, we find a single eigenvalue of positive real part and a second eigenvalue equal to zero. The corresponding center eigendirection is found to be tangent to $\langle 1, 0 \rangle$. Therefore, we may assume a power series representation for the center manifold,

$$v = h(u) = a_1(u - U_2)^2 + a_2(u - U_2)^3 + \dots$$

Inserting this into the differential equation for v , we find

$$a_1 = -\frac{kU_2}{cF},$$

and therefore, the center manifold is locally quadratic. Using this quadratic representation in the differential equation for u we may derive asymptotic decay rates along the slow manifold. In particular, we find

$$u(\xi) = U_2 + \frac{cF}{kU_2\xi} \quad \text{as} \quad \xi \rightarrow -\infty.$$

This is consistent with the known asymptotic decay rate for Fisher-type equations, see [38] for example.

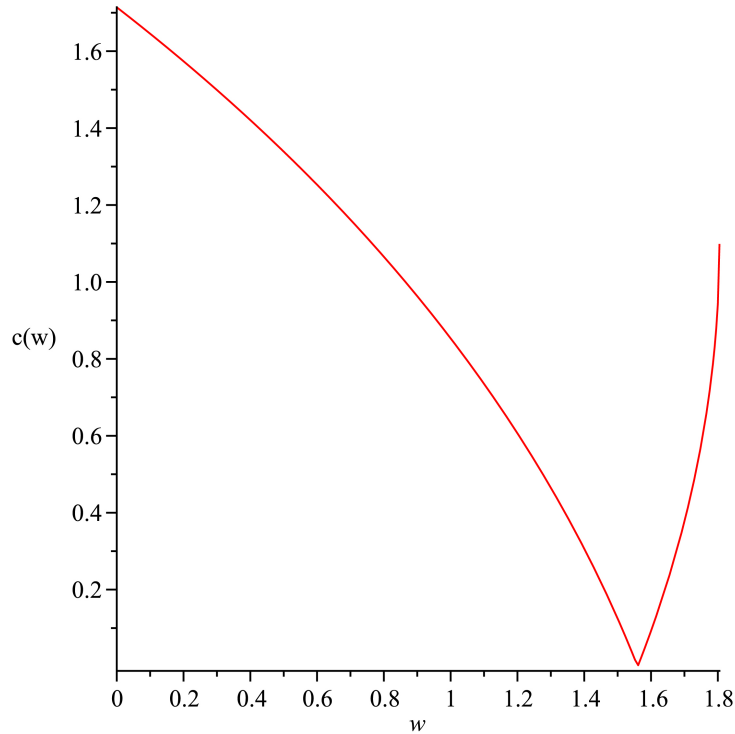


Figure 1: A typical graph of wavespeed for the front and back of the wave, with $M = 1$, $c_1 = 10$, $k = 8$ and $a = .05$. Note that $w_{zero} = 1.56$ and $w_{knee} = 1.805$. The reduced model admits traveling front solutions for $w_f \in [0, 1.56]$ and traveling back solutions for $w_b \in [1.56, 1.805]$. Here $w_{crit} \approx .766$. Note that this picture is typical of the homoclinic orbits that we study – no value of $w \in [w_{zero}, w_{knee}]$ leads to a singular connection between \mathcal{S}_R and \mathcal{S}_L . Therefore the jump back must occur at the knee.

Remark 5. For values w_b satisfying $w_{zero} < w_b < w_{knee}$, we may again use (3.7) and find that the wave speed of the back is described by

$$c(w_b) = \frac{\sqrt{2k}}{F(w_b)} \left(U_1 - \frac{U_2}{2} \right).$$

For the back, we need $\alpha > 0$ to ensure positivity of the wave speed. As is illustrated in figure 1, we observe that below a particular value of w , there exists no choice of w_b for which such a connection between the left slow manifold and right slow manifold can be found. We will label this value of w as w_{crit} . It is defined by the condition that

$$c(w_{crit}) = c_{crit}.$$

Remark 6. We focus only on those homoclinics for which the back departs from the knee with non-critical speed. Traveling pulse solutions for which the back departs the right slow manifold at a point below the knee also exist, i.e. when $c_{crit} > c(0)$. The existence analysis in this case reduces to standard geometric singular perturbation techniques similar to those used for the Fitz-Hugh Nagumo equations [18]. We focus on the knee type homoclinics because they introduce mathematical challenges not yet directly addressed by geometric singular perturbation theory. In addition, the slow algebraic decay of the back is typical of cardiac models so these pulses are of more natural interest.

3.1.4 Summary of the Singular Solution

The singular solution consists of solutions of the fast reduced problems concatenated with sets of fixed points on the slow manifolds. We start with the front which is the heteroclinic connection (3.8) from the left critical manifold $U = 0$ to the right critical manifold $U_2(w)$ located in the plane $w = 0$. To this, we concatenate the

set of fixed points on the critical manifold \mathcal{S}_R between $w = 0$ and $w = w_{knee}$. Third is the the heteroclinic connection between \mathcal{S}_R and \mathcal{S}_L that departs along the center-unstable manifold. Finally, the singular solution consists of those points on \mathcal{S}_L between w_{knee} and $w = 0$. The singular solution is plotted in figure 2.

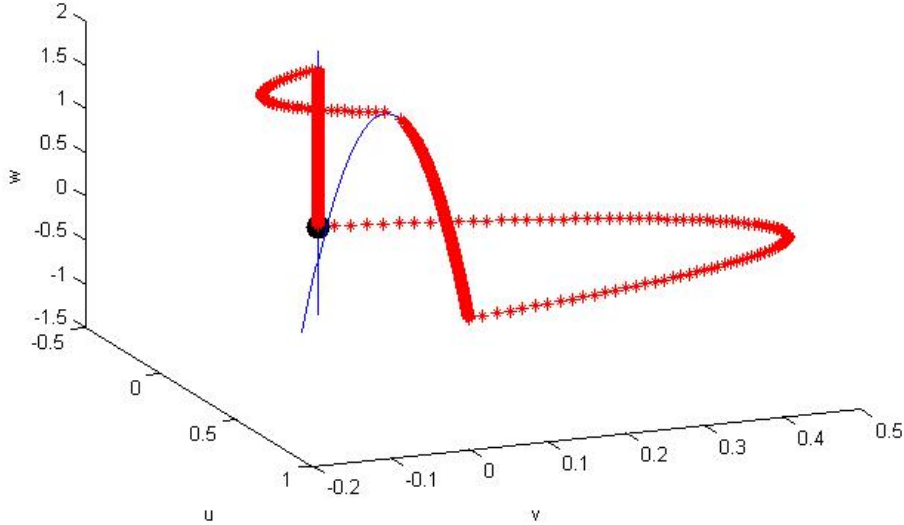


Figure 2: The singular solution for the traveling wave. Here we have taken $M = 0$, $c_1 = 10$, $k = 8$ and $a = .05$. The thin curves represent the slow manifolds to leading order. The large dot is the fixed point at the origin.

3.2 Persistence of the pulse

We now demonstrate that the singular pulse described above persists for small, positive ϵ . We will show that this singular solution lies in the transverse intersection of the stable and unstable manifolds of the origin when $\epsilon = 0$. To do this, we will track the center-unstable manifold of the origin, which we will label \mathcal{M} , forward along the singular orbit and show that it intersects transversely the stable manifold of the origin tracked backwards. Because it lies in the transverse intersection of invariant manifolds, the traveling pulse solution is unique up to translation.

We expect the wavespeed of the traveling wave to be $\mathcal{O}(\epsilon)$ close to the wavespeed selected by the front. Therefore, the first step is to augment our traveling wave system with a trivial differential equation for the wave speed c ,

$$\begin{aligned}
 u' &= F(w)v \\
 v' &= cF^2(w)v + kF(w)u(u-a)(u-1) + uwF(w) \\
 w' &= \frac{\epsilon}{c}(ku - w) \\
 c' &= 0.
 \end{aligned} \tag{3.11}$$

We now break our analysis into pieces, studying the individual jumps between slow manifolds and subsequent slow motions along those manifolds.

3.2.1 Persistence of the front as a fast heteroclinic jump

The first such piece will correspond to the fast jump from the left slow manifold at the origin to the right slow manifold. We will show that the center-unstable manifold emanating from the origin intersects transversely

the center-stable manifold of the right slow manifold in the plane $w = 0$. We will use differential forms to show this intersection is transverse, see [18].

Along the front, the reduced variational equations are given by

$$\begin{aligned}\delta u' &= F(0)\delta v \\ \delta v' &= cF^2(0)\delta v + F(0)f_u(u_f, 0)\delta u + F^2(0)v\delta c \\ \delta c' &= 0,\end{aligned}$$

where we recall the definition of $f(u, w)$ in (2.1). Here, the $\delta u(\eta)$ is a differential one-form acting on η , an element of the tangent space. Therefore, derivatives apply to the vector η and not to the actual one-form. The relevant stable and unstable manifolds are given by

$$\begin{aligned}T_{(u,v,c)}W^{cu}(0, 0, c^*) &= \text{span} \{ \langle v, cF(0)v + f_u(u_f, 0), 0 \rangle, \langle 0, h^+, 1 \rangle \} \\ T_{(u,v,c)}W^{cs}(1, 0, c^*) &= \text{span} \{ \langle v, cF(0)v + f_u(u_f, 0), 0 \rangle, \langle 0, h^-, 1 \rangle \}.\end{aligned}$$

We will refer to n as the tangent vector to the solution and we will let $\eta^+ = \langle 0, h^+, 1 \rangle$ and $\eta^- = \langle 0, h^-, 1 \rangle$ for convenience. Since both manifolds share a common solution, they will share the tangent vector $n = \langle v, cF(0)v + f_u(u_f, 0), 0 \rangle$ following this solution. We define the following differential two forms

$$\begin{aligned}P_{uv} &= \delta u \wedge \delta v \\ P_{vc} &= \delta v \wedge \delta c \\ P_{uc} &= \delta u \wedge \delta c.\end{aligned}$$

These two forms are bi-linear functionals on the tangent space. Their arguments are vectors that span a plane in \mathbb{R}^3 . When normalized appropriately, these quantities measure the area of the projection of the tracked plane onto the respective coordinate plane (i.e. the $u - v$ coordinate plane for P_{uv}).

At the point of intersection, the two manifolds will intersect transversely if there is no choice of $\alpha \in \mathbb{R}$ such that,

$$\langle P_{uv}(n, \eta^+), P_{vc}(n, \eta^+), P_{uc}(n, \eta^+) \rangle = \alpha \langle P_{uv}(n, \eta^-), P_{vc}(n, \eta^-), P_{uc}(n, \eta^-) \rangle,$$

i.e., they are linearly independent. We verify this by computing the differential equations associated to these differential 2-forms. Namely,

$$\begin{aligned}P'_{uv} &= cF(0)^2 P_{uv} + F^2(0)vP_{uc} \\ P'_{vc} &= cF(0)^2 P_{vc} + F(0)f_u(u_f, 0)P_{uc} \\ P'_{uc} &= F(0)P_{vc}.\end{aligned}$$

We can compute explicitly that $P_{uc}(n, \eta^+) = P_{uc}(n, \eta^-) = v$. We also note that $P_{uv}(n, \eta^\pm) = vh^\pm$. Therefore, if $h^+ \neq h^-$, we will have shown local transversality of these two manifolds. We proceed as follows: first, we use the fact that $P_{uc} = v$ to reduce the first variational equation to

$$P'_{uv} = cF^2(0)P_{uv} + F^2(0)v^2.$$

This is solved as

$$P_{uv} = F^2(0)e^{cF^2(0)\xi} \int_{-\infty}^{\xi} (e^{-cF^2(0)\tau} v^2(\tau)) d\tau.$$

Since all terms are positive, we conclude that

$$P_{uv}(n, \eta^+) = vh^+ > 0.$$

Positivity of $v(\xi)$ implies that $h^+ > 0$. For the manifold W^{cs} , we perform an analogous computation to find that

$$P_{uv} = -F^2(0)e^{cF^2(0)\xi} \int_{\xi}^{\infty} (e^{-cF^2(0)\tau} v^2(\tau)) d\tau,$$

from which we deduce that $h^- < 0$. Therefore, the two manifolds intersect transversely.

3.2.2 Persistence of the segment near the right slow manifold

We will now track \mathcal{M} as it passes the right slow manifold. This will require two steps. First, we track \mathcal{M} to a neighborhood of the non-hyperbolic knee using the Exchange Lemma. Then, we use center manifold theory and geometric desingularization to track this manifold through a neighborhood of the knee.

Recall the coordinates of the knee,

$$(u, v, w, c) = \left(\frac{1+a}{2}, 0, \frac{k}{4}(1-a)^2, c(0) \right),$$

for which we designate $w_{knee} = \frac{k}{4}(1-a)^2$ and $u_{knee} = \frac{1+a}{2}$. For any $\delta > 0$ define a δ neighborhood of the knee by,

$$\mathcal{K} = \{(u, v, w, c) \mid |u - u_{knee}| < \delta, |v| < \delta, |w - w_{knee}| < \delta, |c - c(0)| < \delta\}.$$

Let $b_r = \mathcal{S}_R \cap \partial\mathcal{K}$. We have the following result.

Lemma 3.1. *For fixed $\delta > 0$, the tracked manifold \mathcal{M} is $C^1, \mathcal{O}(\epsilon)$ close to $W^{cu}(\mathcal{S}_R)$ in a neighborhood of b_r .*

Proof: We have that \mathcal{M} intersects $W^{cs}(\mathcal{S}_R)$ transversely on entry into a neighborhood of \mathcal{S}_R . The proof is then a standard application of the Exchange Lemma, [19]. ■

We now focus on the dynamics in \mathcal{K} . Append to (3.11) a trivial equation for ϵ . Since c has been fixed to leading order by the front, we ignore the trivial equation for c . Then the point $(u, v, w, \epsilon) = (u_{knee}, 0, w_{knee}, 0)$ is a fixed point for the flow. This fixed point is center-unstable, with one unstable eigenvalue and three zero eigenvalues. We have the following,

Lemma 3.2. *For any $k > 0$, there exists a local C^k center manifold \mathcal{C}_{knee} of $(u_{knee}, 0, w_{knee}, 0)$, which can be given as a graph,*

$$v = h(u, w, \epsilon) = b_{200}(u - u_{knee})^2 + b_{010}(w - w_{knee}) + \mathcal{O}(\epsilon, (w - w_{knee})^2, (u - u_{knee})(w - w_{knee})).$$

There exists $b > 0$ and independent of ϵ , for which the reduced dynamics on \mathcal{C}_{knee} are

$$\begin{aligned} u_\xi &= -b(u - u_{knee})^2 - \frac{u_{knee}}{c}(w - w_{knee}) + \mathcal{O}(\epsilon, (w - w_{knee})^2, (u - u_{knee})(w - w_{knee}), (u - u_{knee})^3) \\ w_\xi &= \epsilon \left(\frac{ku_{knee}}{c} - \frac{w_{knee}}{c} \right) + \mathcal{O}(\epsilon, (w - w_{knee})^2, (u - u_{knee})(w - w_{knee}), (u - u_{knee})^3) \\ \epsilon_\xi &= 0. \end{aligned} \tag{3.12}$$

In addition, to each point $p \in \mathcal{C}_{knee}$ there exists an associated, C^k one dimensional unstable fiber $\mathcal{F}_u(p)$ given as a graph over the unstable eigenvector $\langle 1, cF^2(w_{knee}), 0, 0 \rangle$.

Proof. See Appendix A ■

If δ is sufficiently small, then \mathcal{M} and \mathcal{C}_{knee} intersect transversely. Locally, the flow of each point in \mathcal{M} can be decomposed into the flow of a basepoint in \mathcal{C}_{knee} and a point in the unstable fiber of that basepoint. The flow of the basepoints in the center manifold is equivalent to the normal form for a fold point studied in [23]. We define the entrance and exit sets,

$$\begin{aligned} \Delta^{in} &= \{(u, w, \epsilon) \mid w = w_{knee} - \rho^2\} \\ \Delta^{out} &= \{(u, w, \epsilon) \mid u = u_{knee} - \rho\}, \end{aligned}$$

where $\rho > 0$. We apply verbatim a theorem of [23].

Theorem 2. *Let $\pi : \Delta^{in} \rightarrow \Delta^{out}$ be the transition map for the flow of (3.12). Then for all $\epsilon \in [0, \epsilon_0]$ we have,*

1. The manifold $S_{a,\epsilon}$ passes through Δ^{out} at a point $(u, w, \epsilon) = (u_{knee} - \rho, w_{knee} + h(\epsilon), \epsilon)$ with $h(\epsilon) = \mathcal{O}(\epsilon^{2/3})$.
2. The transition map π is a contraction with contraction rate $\mathcal{O}(e^{-C/\epsilon})$ with C a positive constant.

This leads to the following result.

Lemma 3.3. *In a neighborhood of $(u, v, w) = (u_{knee} - \rho, h(u_{knee} - \rho, w_{knee}), 0), w_{knee})$, \mathcal{M} is C^1 , $\mathcal{O}(\epsilon^{2/3})$ close to the plane $w = w_{knee}$.*

Proof. We establish the C^0 result first. Recall that \mathcal{M} is C^1 $\mathcal{O}(\epsilon)$ close to the smooth manifold $W^{cu}(\mathcal{S}_R)$ on entry to \mathcal{K} . For each ϵ sufficiently small, this guarantees the existence of a unique $p^{in} = \mathcal{M} \cap \mathcal{C}_{knee} \cap \Delta^{in}$. Near p^{in} , the dynamics of each point in \mathcal{M} can be decomposed into the flow of a basepoint $p \in \mathcal{C}_{knee}$ and an expansion in the corresponding unstable fiber $\mathcal{F}_u(p)$. Theorem 2 implies that, on exit from \mathcal{K} , all of the basepoints exit \mathcal{K} $\mathcal{O}(e^{-C/\epsilon})$ close to πp^{in} or $(u, w, \epsilon) = (u_{knee} - \rho, w_{knee} + h(\epsilon), \epsilon)$. Since the fibers depend smoothly on their basepoints, the exponential contraction of π implies that each unstable fiber will be locally $\mathcal{O}(\epsilon^{2/3})$ close to the unstable fiber at $(u, w, \epsilon) = (u_{knee} - \rho, w_{knee}, 0)$. Since the unstable fibers are given as a graph over the unstable eigenvector, whose w component is zero, we have the C^0 closeness result.

We now turn to the C^1 result. We make the following change of coordinates,

$$\tilde{v} = v - h(u, w, \epsilon), \quad \tilde{u} = u - u_{knee}, \quad \tilde{w} = w - w_{knee}.$$

In these coordinates, the equation is

$$\begin{aligned} \tilde{u}_\xi &= F(\tilde{w} + w_{knee})(\tilde{v} + h(u, w, \epsilon)) \\ \tilde{v}_\xi &= cF^2(\tilde{w} + w_{knee})\tilde{v} \\ \tilde{w}_\xi &= \epsilon \left(\frac{k(\tilde{u} + u_{knee})}{c} - \frac{\tilde{w} + w_{knee}}{c} \right) \\ \epsilon_\xi &= 0. \end{aligned}$$

We track the tangent space as it evolves along the trajectory through p^{in} (where $\tilde{v} = 0$). The variational equation along this orbit has a simplified form,

$$\begin{aligned} \delta\tilde{u}' &= F(\tilde{w} + w_{knee})(\delta\tilde{v} + \nabla h \cdot \langle \delta\tilde{u}, \delta\tilde{w} \rangle) + F'(\tilde{w} + w_{knee})h(u, w, \epsilon)\delta\tilde{w} \\ \delta\tilde{v}' &= cF^2(\tilde{w} + w_{knee})\delta\tilde{v} \\ \delta\tilde{w}' &= \frac{\epsilon k}{c}\delta\tilde{u} - \frac{\epsilon}{c}\delta\tilde{w}. \end{aligned}$$

The $\delta\tilde{v}$ equation has an explicit solution and the subspace $\delta\tilde{v} = 0$ is invariant. Restricted to this subspace, we find exactly the variational equation for the center manifold.

$$\begin{aligned} \delta\tilde{u}' &= F'(w)h(u, w, \epsilon)\delta\tilde{w} + 2F(w)b_{200}(u - u_{knee})\delta\tilde{u} + b_{010}F(w)\delta\tilde{w} + \eta(\epsilon, w, u, \delta\tilde{u}, \delta\tilde{w}) \\ \delta\tilde{w}' &= \frac{\epsilon k}{c}\delta\tilde{u} - \frac{\epsilon}{c}\delta\tilde{w}, \end{aligned}$$

where $\eta = \mathcal{O}(\epsilon, (w - w_{knee})\delta\tilde{w}, (w - w_{knee})\delta\tilde{u}, (u - u_{knee})\delta\tilde{w})$. At p^{in} , the tangent space of \mathcal{M} is $\mathcal{O}(\epsilon)$ close to the span of the vectors $\eta_1 = \langle 1, \frac{cF^2(w_{knee} - \rho^2)}{2} + \frac{1}{2}\sqrt{c^2F^4 + 4(f_U(U_2(w_{knee} - \rho^2), w_{knee} - \rho^2))}, 0 \rangle$ and $\eta_2 = \langle 1, 0, -2ku + k(1+a) \rangle$. Let η_c be the restriction of this plane to the tangent space of \mathcal{C}_{knee} at p^{in} . We now consider the differential two forms P_{uv} , P_{uw} and P_{vc} acting on the vectors η_1 and η_c . Then,

$$\begin{aligned} P_{uv}(\eta_1, \eta_c) &= \delta\tilde{v}(\eta_1)\delta\tilde{u}(\eta_c) \\ P_{vw}(\eta_1, \eta_c) &= \delta\tilde{v}(\eta_1)\delta\tilde{w}(\eta_c) \\ P_{uw}(\eta_1, \eta_c) &= \delta\tilde{u}(\eta_1)\delta\tilde{w}(\eta_c) - \delta\tilde{u}(\eta_c)\delta\tilde{w}(\eta_1). \end{aligned}$$

Normalize these two-forms by $\hat{P}_\sigma = \frac{P_\sigma}{P_{uv}}$. The second statement in Theorem 2 implies that vectors transverse to the flow are contracted by an exponential amount. Since η_c is close to direction of the flow at p^{in} exits \mathcal{K} exponentially close to the vector pointing in the direction of the flow. This gives $\frac{\delta\tilde{w}(\eta_c)}{\delta\tilde{u}(\eta_c)} = \mathcal{O}(\epsilon)$. Then we have $\hat{P}_{uv} = 1$, $\hat{P}_{vw} = \mathcal{O}(\epsilon)$ and $\hat{P}_{uw} = \mathcal{O}(\epsilon)$. This establishes the C^1 result. ■

3.2.3 Conclusion of the proof of Theorem 1

We have now tracked \mathcal{M} to an $\mathcal{O}(1)$ distance from the non-hyperbolic knee and shown that it is C^1 , $\mathcal{O}(\epsilon^{2/3})$ close to the plane $w = w_{knee}$. Due to the slow w dynamics, this result will still hold as \mathcal{M} enters an $\mathcal{O}(1)$ neighborhood of \mathcal{S}_L . We then compare \mathcal{M} with the stable manifold of \mathcal{S}_L . Due to Fenichel Theory, the stable manifold is tangent to the stable eigenspace of \mathcal{S}_L . It is easy to verify that this eigenspace has non-zero w component and therefore it must intersect transversely with \mathcal{M} . This establishes Theorem 1.

3.3 Further information concerning the decomposition of the wave

We conclude the existence analysis with the following decomposition that will be crucial for the stability analysis. The idea is that at each point the actual solution can always be described as either pointwise (in ξ) close to the singular solution or evolving at an $\mathcal{O}(\epsilon)$ rate. To begin, we will decompose \mathbb{R} into five intervals corresponding to different pieces of the solution. Without loss of generality fix $\xi = 0$ to be the unique point where the wave satisfies $u(\xi, \epsilon) = 1/2$ and $w < 1/2$. Now we will define $\xi_r(\epsilon), \xi_k(\epsilon), \xi_b(\epsilon), \xi_l(\epsilon)$ to be values for which the wave transitions from being primarily described by one piece of the singular solution to the next. For example, $\xi_r(\epsilon)$ describes the value of ξ for which the wave transitions from being described primarily by the dynamics of the reduced front to where the dynamics are predominately described by the right slow manifold.

Lemma 3.4. *For a particular translate of the homoclinic solution derived in Theorem 1, there exists values of the traveling wave coordinate ξ such that the wave profile has the following characterization,*

1. On $J_f := (-\infty, \xi_r(\epsilon))$ and $J_b := (\xi_b(\epsilon), \xi_l(\epsilon))$ the solution satisfies

$$\begin{aligned} (u(\xi, \epsilon), w(\xi, \epsilon)) &= (U_f(\xi) + \epsilon \log(\epsilon)U_1(\xi, \epsilon), W_f + \epsilon \log(\epsilon)W_1(\xi, \epsilon)), \\ (u(\xi, \epsilon), w(\xi, \epsilon)) &= (U_b(\xi) + \epsilon^{1/3}U_1(\xi, \epsilon), W_b + \epsilon^{1/3}W_1(\xi, \epsilon)) \end{aligned}$$

with $U_1 = \mathcal{O}(1)$ and $W_1 = \mathcal{O}(1)$.

2. On $J_r := (\xi_r(\epsilon), \xi_k(\epsilon))$ and $J_l := (\xi_l(\epsilon), \infty)$, we have,

$$\frac{\partial}{\partial \xi} U(\xi, \epsilon) = \mathcal{O}(\epsilon), \quad \frac{\partial}{\partial \xi} W(\xi, \epsilon) = \mathcal{O}(\epsilon).$$

3. On $J_k := (\xi_k, \xi_b)$ we have

$$(u, w) = (\Gamma, \Omega) + \mathcal{O}(\epsilon^{1/3}).$$

Proof: This decomposition is a consequence of the geometric techniques employed in the existence analysis, namely Fenichel Theory and geometric desingularization. The tools necessary for the proof can be found in Appendix B. ■

4 Statement of the Main Stability Result

In this section, we will study the spectral stability of the traveling pulse solution constructed in Theorem 1. We will linearize the system and study the behavior of solutions that are a small perturbation of the traveling pulse. We will establish the following result.

Theorem 3. *For each $(k, a, c_1, M) \in \Pi$, there exists $\epsilon_2 > 0$ such that for all $0 < \epsilon < \epsilon_2$, the traveling pulse solution from Theorem 1 is spectrally stable with a simple zero eigenvalue at $\lambda = 0$ due to translational invariance of the pulse.*

Denoting with capital letters the pulse constructed in Theorem 1, we linearize by letting $u(\xi, t) = U(\xi) + p(\xi, t)$ and $w(\xi) = W(\xi) + r(\xi, t)$, substitute these into (3.1) and neglect nonlinear terms,

$$\begin{aligned} p_t &= \frac{1}{F} \frac{\partial}{\partial \xi} \left(\frac{1}{F} p' \right) - cp' - f_U(U, W)p - f_W(U, W)r - \left(\frac{F_W}{F^2} \frac{\partial U'}{\partial \xi} \right) r - \frac{1}{F} \frac{\partial}{\partial \xi} \left(\frac{F_W U'}{F^2} r \right) \\ r_t &= -cr' + \epsilon(kp - r), \end{aligned} \quad (4.1)$$

where we recall $f(u, w) = ku(u - a)(u - 1) + uw$. The right hand side of this partial differential equation defines a linear operator \mathcal{L} acting on the vector $(p, r)^T$. We will seek values of λ for which bounded solutions of the linearized eigenvalue problem $\mathcal{L} - \lambda I = 0$ exist.

The linearized eigenvalue problem is an ordinary differential equation in ξ . It may be written as a system of first order equations as follows,

$$\begin{aligned} p' &= F(W)q \\ q' &= F(W)(f_U(U, W) + \lambda)p + cF^2(W)q + F(W)f_W(U, W)r + \left(\frac{F_W}{F} \frac{\partial U'}{\partial \xi} \right) r + \frac{\partial}{\partial \xi} \left(\frac{F_W U'}{F^2} r \right) \\ r' &= \frac{k\epsilon}{c}p - \frac{\lambda + \epsilon}{c}r. \end{aligned} \quad (4.2)$$

Remark 7. *The derivative terms in the right hand side of the equation for q are given by*

$$\begin{aligned} \left(\frac{F_W}{F} \frac{\partial U'}{\partial \xi} \right) r + \frac{\partial}{\partial \xi} \left(\frac{F_W U'}{F^2} r \right) &= \frac{1}{F^2} \left(2F_W U'' - 3 \frac{F_W^2 U' W'}{F} + F_{WW} U' W' \right. \\ &\quad \left. - \frac{(\lambda + \epsilon) F_W U'}{c} \right) r + \frac{\epsilon k F_W U'}{c F^2} p. \end{aligned}$$

We will often denote the right hand side of system (4.2) by $A(\xi, \lambda, \epsilon)$. In this way, the linearized eigenvalue problem is equivalent to the system,

$$\frac{dx}{d\xi} = A(\xi, \lambda, \epsilon)x. \quad (4.3)$$

Since they satisfy a linear non-autonomous system with well-defined limits as $\xi \rightarrow \pm\infty$, the solutions to this differential equation can be characterized in terms of exponential dichotomies. Exponential dichotomies generalize the notion of hyperbolicity to non-autonomous systems. The linear system on \mathbb{C}^n , is said to possess an exponential dichotomy on an interval J if there exist $K, L > 0$, $\alpha, \beta > 0$ and a linear projection $P(\xi) : \mathbb{R} \times \mathbb{C}^n \rightarrow \mathbb{C}^n$ satisfying $P^2 = P$ such that the following conditions hold:

$$\begin{aligned} X(\xi_2, \xi_1)P(\xi_1) &= P(\xi_2)X(\xi_2, \xi_1) \\ |X(\xi_2, \xi_1)P(\xi_1)| &\leq K e^{-\alpha(\xi_2 - \xi_1)} \quad \text{for } \xi_2 \geq \xi_1, \quad \xi_1, \xi_2 \in J \\ |X(\xi_2, \xi_1)(1 - P(\xi_1))| &\leq L e^{-\beta(\xi_1 - \xi_2)} \quad \text{for } \xi_1 \geq \xi_2, \quad \xi_1, \xi_2 \in J. \end{aligned} \quad (4.4)$$

Here X denotes the fundamental matrix solution of (4.3). The interval J is typically taken to be either \mathbb{R} , \mathbb{R}^+ or \mathbb{R}^- . We note that on \mathbb{R}^+ , the range of P is chosen uniquely as the space of all initial data that converges exponentially to zero as $\xi \rightarrow \infty$. The nullspace of this projection operator is not unique however. Likewise, on \mathbb{R}^- it is the nullspace of the projection operator $(1 - P)$ that is uniquely determined as the space of initial data converging exponentially to zero in backwards time. Only on \mathbb{R} are the range and nullspace of P both chosen uniquely. The Morse index of an exponential dichotomy measures the dimension of the null space of the stable projection. When the exponential dichotomy is posed on a half line, we refer to i_+ and i_- as the Morse indices of the exponential dichotomies on either half line. Since we are only concerned with the case of traveling pulses which are homoclinic orbits in (4.3), we have that $i_+ = i_-$. Exponential dichotomies can be used to whenever there exists a gap between the exponential rates on two different subspaces. In this way, it is not necessary that α and β always be positive, but only that $-\alpha < \beta$. Exponential dichotomies and properties ensuring their existence have been studied in great detail. We have collected some relevant Theorems in Appendix C.

Spectral properties of \mathcal{L} , namely invertibility of $\mathcal{L} - \lambda$ in a Banach Space, can be restated in terms of properties of exponential dichotomies of (4.3). In particular, the spectrum of $\sigma(\mathcal{L})$ can be characterized by (see [28, 29]):

- λ is in the resolvent set if and only if (4.3) has an exponential dichotomy on \mathbb{R} .
- λ is in the essential spectrum if $A_\infty := \lim_{\xi \rightarrow \pm\infty} A(\xi, \lambda)$ is not hyperbolic, or if A_∞ is hyperbolic but the Morse indices are not equal, i.e. $i_+ \neq i_-$.
- λ is in the point spectrum if (4.3) has exponential dichotomies on both \mathbb{R}^+ and \mathbb{R}^- but not on \mathbb{R} . In other words, letting P^+ be the stable projection for \mathbb{R}^+ and letting P^- be the stable projection for \mathbb{R}^- we have that

$$\text{rng}(P^+) \cap \ker(P^-) \neq \emptyset.$$

Given this characterization, the essential spectrum can be located using only information about the asymptotic system A_∞ . The point spectrum is more elusive. We will make use of the Evans Function,

$$D(\lambda) = \text{rng}P^+(0) \wedge \text{rng}(1 - P^-(0)), \quad (4.5)$$

see Chapter 4 in [34]. The Evans function is an analytic function defined on the complement of the essential spectrum having zeros for values of λ in the point spectrum. In addition, the order of λ as a zero of $D(\lambda)$ corresponds to the algebraic multiplicity of the eigenvalue. The analyticity of $D(\lambda)$ is the key feature, as arbitrarily small analytic perturbations of $D(\lambda)$ will retain the same number of zeros.

5 Preliminary Spectral Analysis

5.1 The essential spectrum

We begin our analysis of the spectrum by computing the essential spectrum. Recall that the essential spectrum is characterized by the values of λ for which the asymptotic matrix A_∞ has eigenvalues on the imaginary axis. Here,

$$A_\infty(\lambda) = \begin{pmatrix} 0 & 1 + \frac{M}{2c_1} & 0 \\ (ka + \lambda)(1 + \frac{M}{2c_1}) & c(1 + \frac{M}{2c_1})^2 & 0 \\ \frac{\epsilon k}{c} & 0 & -\frac{\lambda + \epsilon}{c} \end{pmatrix}.$$

Thus,

$$\sigma_{ess} = \{icl - \epsilon : l \in \mathbb{R}\} \cup \left\{ -\frac{l^2}{(1 + \frac{M}{2c_1})^2} - icl - ka : l \in \mathbb{R} \right\}. \quad (5.1)$$

The essential spectrum is plotted in Figure 3. The quadratic part, which has a vertex at $\lambda = -ka$, is always bounded strictly in the left half plane. The vertical component will converge to the imaginary axis as $\epsilon \rightarrow 0$. We also note that for $\lambda = 0$, the fixed point at $(p, q, r) = (0, 0, 0)$ has one positive eigenvalue and two negative eigenvalues for all λ with $\text{Re}(\lambda) > -\epsilon$.

5.2 The reduced spectra along the front and back

The spectra of the reduced problems along the front and the back will be of critical importance as we construct the Evans Function for the full system. We will discuss the case of the front first. Recall that the reduced problem along the front is given by setting $\epsilon = 0$ in (3.1). In this case, we have that w is a constant, which along the front is given by $w = 0$. The equation for u is

$$\frac{\partial^2 u}{\partial \xi^2} - cF^2(0) \frac{\partial u}{\partial \xi} - F^2(0)ku(u - a)(u - 1) = 0.$$

The reduced linear eigenvalue problem along the front is given by

$$\mathcal{L}^f p := \frac{\partial^2 p}{\partial \xi^2} - cF^2(0) \frac{\partial p}{\partial \xi} - F^2(0)f_U(U_f(\xi), 0)p = \lambda p.$$

The spectrum of this Sturm-Liouville operator has been studied in [12], where it was shown that the spectrum of \mathcal{L}^f has an isolated eigenvalue with algebraic multiplicity one at $\lambda = 0$. Therefore, we may define a reduced

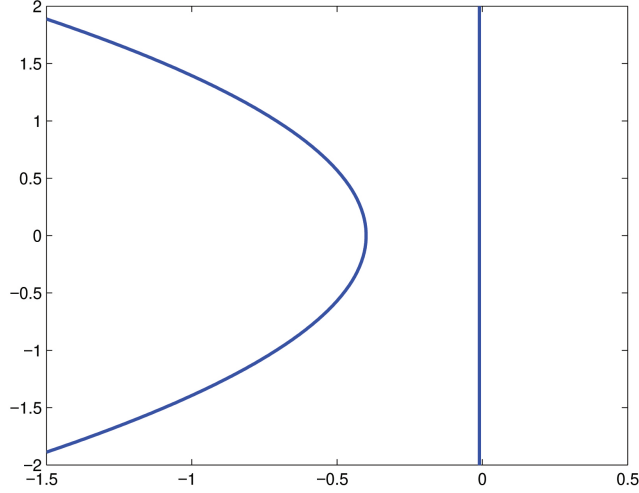


Figure 3: An illustration of (5.1), the boundary of the essential spectrum in the complex plane. The parameters used here are $\epsilon = .01$, $k = 8$, $a = .05$, $c_1 = 10$ and $M = 1$.

Evans function for the front, $D_F(\lambda)$. This function is analytic on a region that includes all of the right half of the complex plane as well as a vertical strip of the left half-plane. $D_F(\lambda)$ has a simple zero at $\lambda = 0$. All other zeros lie in the left-half plane.

Analogously, the reduced equation along the back is given by,

$$\frac{\partial^2 u}{\partial \xi^2} - cF^2(W_b) \frac{\partial u}{\partial \xi} - F^2(W_b)ku(u - U_2(W_b))^2 = 0.$$

The linearized eigenvalue problem for the reduced problem along the back is given by

$$\mathcal{L}^b p := \frac{\partial^2 p}{\partial \xi^2} - cF^2(W_b) \frac{\partial p}{\partial \xi} - F^2(W_b)f_U(U_b(\xi), W_b)p = \lambda p.$$

The spectrum of this operator was studied in [37]. The boundary of the essential spectrum is again given by the values of λ for which the limiting system has purely imaginary eigenvalues. Since $f_U = 0$ at the knee, we get that the set $\{-l^2 + icF^2(W_b)l : l \in \mathbb{R}\}$ is one such curve (the other curve lies strictly in the stable half-plane). As a result, we have that $\lambda = 0$ is an element of the essential spectrum of \mathcal{L}^b . The derivative of the wave $\partial_\xi U_b(\xi)$ solves the linearized eigenvalue problem at $\lambda = 0$. This solution connects the center-unstable subspace at $\xi = -\infty$ to the stable subspace at $\xi = \infty$. Thus, one finds that the unstable subspace is preserved. The authors in [37] defined an Evans function $D_B(\lambda)$ for the reduced problem along the back. This analytic Evans function is non-zero to the right of the essential spectrum of the back. Using exponential weights, one finds that there exists an analytic extension of $D_B(\lambda)$ into the essential spectrum. This analytic extension was found to be non-zero for all values of λ in a suitable neighborhood of the origin. At first glance one may expect an embedded eigenvalue at $\lambda = 0$ due to the derivative of the reduced wave profile satisfying the eigenvalue equation. This is not the case however as the Evans function measures connections between the unstable subspace at $\xi = -\infty$ and the stable subspace at $\xi = \infty$. The derivative of the wave U'_b connects the center-unstable subspace at $\xi = -\infty$ to the stable subspace at $\xi = \infty$. In this way, the unstable connection is seen to exist for all λ in a neighborhood of the origin.

5.3 The regime of large $|\lambda|$

In this section, we show the non-existence of point spectrum for the eigenvalue problem when $\text{Re } \lambda > -\epsilon$ and $|\lambda|$ large. This will allow us to restrict to a compact subset of the complex plane in the analysis of

section 6. For values of λ in this compact set, we will be able to select the constants for our exponential dichotomies in a consistent, $\mathcal{O}(1)$ manner. The fact that λ which are large in modulus do not contribute to the spectrum is well established. Evans proved a result along these lines in his original work [10]. We will follow a similar argument of Sandstede, see Section 4.2.2 of [34]. The key idea is that as λ becomes large in modulus, it dominates the stability problem and it is no longer possible to have a solution that is bounded in both asymptotic limits.

To see this, we rescale the linearized eigenvalue problem (4.2) as

$$\tau = \sqrt{|\lambda|}\xi, \quad P = p, \quad Q = \frac{q}{\sqrt{|\lambda|}}, \quad R = r.$$

This transforms (4.2) into

$$\begin{aligned} \dot{P} &= F(W)Q \\ \dot{Q} &= \frac{\lambda}{|\lambda|}F(W)P + \mathcal{O}\left(\frac{1}{\sqrt{|\lambda|}}\right) \\ \dot{R} &= \frac{-\lambda}{c\sqrt{|\lambda|}}R + \mathcal{O}\left(\frac{\epsilon}{\sqrt{|\lambda|}}\right). \end{aligned} \tag{5.2}$$

Neglecting the higher order terms, the linearized eigenvalue problem at $\tau = \pm\infty$ is hyperbolic with eigenvalues $\pm\sqrt{\frac{\lambda}{|\lambda|}}F(0)$ and $-\frac{\lambda}{c\sqrt{|\lambda|}}$. Since the only τ dependence in (5.2) to leading order in $\sqrt{|\lambda|}^{-1}$ is through the slowly varying $W(\tau)$, the leading order equation varies slowly in τ and Theorem 9 in Appendix C can be applied to find the existence of an exponential dichotomy on all of \mathbb{R} . Then, Theorem 7 implies that this dichotomy persists for the full system. Recalling our previous discussion, this implies that the Evans function $D(\lambda)$ is non-zero for large λ with $\text{Re}(\lambda) > 0$. For λ on the imaginary axis, the eigenvalue $-\frac{\lambda}{c\sqrt{|\lambda|}}$ becomes imaginary as the essential spectrum is approached. However, it is easy to see that if one is willing to relax the hyperbolicity condition in Theorem 9 the same results apply provided that a spectral gap persists between the stable and unstable eigenvalues. In fact, this argument can be used to analytically extend the Evans function a small distance into the left half plane.

To summarize, we have shown that for all $0 < \epsilon < \epsilon_0$, there exists constants $\mathbf{K} > 0$ and $b > 0$ such that the Evans function has an analytic continuation with $D(\lambda) \neq 0$ for all $|\lambda| \geq \mathbf{K}$ with $\text{Re}(\lambda) > -b$.

5.4 Restriction to a compact set

From this point forward, we are interested in the existence of point spectra in the set

$$\Omega := \{\lambda \in \mathbb{C} | \text{Re}(\lambda) > -\delta, |\lambda| < \mathbf{K}\}.$$

We will remark on the constant δ in a moment. Our proof will ultimately rely on Rouché's Theorem to count the number of zeros of the analytic Evans function $D(\lambda)$ in a neighborhood of the origin. Since the essential spectrum accumulates on the imaginary axis, this necessitates the analytic extension of $D(\lambda)$ into the essential spectrum. As we noted above, such an extension is possible provided a spectral gap between the eigenvalues of $A_\infty(\lambda)$ persists. In fact, it is convenient for the analysis if this spectral gap exists for all values of $\xi \in \mathbb{R}$. We denote the three eigenvalues of $A(\xi, \lambda, \epsilon)$, which may also be referred to as spatial eigenvalues, by,

$$\begin{aligned} \mu_u(\xi, \lambda) &= \frac{cF^2(W)}{2} + \frac{1}{2}\sqrt{c^2F^4 + 4(f_U(U, W) + \lambda)} \\ \mu_s(\xi, \lambda) &= \frac{cF^2(W)}{2} - \frac{1}{2}\sqrt{c^2F^4 + 4(f_U(U, W) + \lambda)} \\ \mu_c(\lambda) &= \frac{-\lambda}{c}. \end{aligned} \tag{5.3}$$

The constant $\delta(k, a, c_1, M)$ will be selected so that the following properties hold:

1. $D_F(\lambda) \neq 0$ for all $\{\lambda | \operatorname{Re} \lambda > -\delta\}$ except at $\lambda = 0$
2. $D_B(\lambda) \neq 0$ for all $\{\lambda | \operatorname{Re} \lambda > -\delta\}$ (see [37])
3. For all $\xi \in \mathbb{R}$, there is a spectral gap between the stable $(\mu_s(\xi, \lambda), \mu_c(\xi, \lambda))$ and unstable $(\mu_u(\xi, \lambda))$ eigenvalues, see (5.3). In particular, we will require

$$0 < \delta < \min \left\{ ka, \frac{k(1+a)^2}{24} \right\}.$$

We recall that $D_F(\lambda)$ and $D_B(\lambda)$ are defined in Section 5.2. Verifying that the final condition on δ implies the existence of a spectral gap will be delayed until the proof of Theorem 3 (see (6.3) and (6.6)).

6 Proof of Theorem 3

In this section, we construct exponential dichotomies that describe the evolution of the linearized eigenvalue problem (4.2) over each of the intervals J_f, J_r, J_k, J_b, J_l defined in section 3.3. These exponential dichotomies will be the fundamental objects used to track the stable and unstable subspaces needed for the Evans function. The proof will draw heavily on well known roughness of dichotomy results, which we have collected in Appendix C.

6.1 Exponential dichotomy for the front

Recall that we have fixed $\xi = 0$ to be the unique value of ξ for which the wave satisfies $u = 1/2$ and $w < 1/2$. For values of $\xi \in J_f = (-\infty, -\theta_f \log(\epsilon))$, Lemma 3.4 implies

$$\begin{aligned} U(\xi) &= U_f(\xi) + \epsilon \log(\epsilon) U_1(\xi, \epsilon) \\ W(\xi) &= W_f + \epsilon \log(\epsilon) W_1(\xi, \epsilon), \end{aligned}$$

where $|U_1|, |W_1| < M_f$, with $M_f(k, a, c_1, M)$ chosen independently of ϵ . Again, let $x = (p, q, r)^T$ and write the linearized eigenvalue equation (4.3) as the system,

$$x' = (A(\xi, \lambda, 0) + B(\xi, \lambda, \epsilon))x. \quad (6.1)$$

where $B(\xi, \lambda, \epsilon) = A(\xi, \lambda, \epsilon) - A(\xi, \lambda, 0)$ for $\xi \in J_f$. In particular,

$$\begin{aligned} A(\xi, \lambda, 0) &= \begin{pmatrix} 0 & F & 0 \\ F(f_U(U_f, W_f) + \lambda) & cF^2 & Ff_W(U_f, W_f) + 2\frac{F_W}{F^2}U_f'' - \frac{\lambda}{cF^2}F_WU_f' \\ 0 & 0 & -\frac{\lambda}{c} \end{pmatrix} \\ B(\xi, \lambda, \epsilon) &= \begin{pmatrix} 0 & F_1 & 0 \\ b_{21} & 2cFF_1 & b_{23} \\ \frac{\epsilon k}{c} & 0 & -\frac{\epsilon}{c} \end{pmatrix} \\ b_{21} &= F_1(f_U + \lambda) + Ff_{UU}U_1 + Ff_{UW}W_1 + \frac{\epsilon k F_W U''}{cF^2} \\ b_{23} &= F_1 f_W - \frac{3F_W U' W'}{F^3} + \frac{F_W W U' W'}{F^2} - \frac{F_W U'}{cF^2}. \end{aligned}$$

Here terms of the form F_1 refer to the first variation of F , i.e. $F_1 = F(W(\xi)) - F(W_f)$. Note that all terms in $B(\xi, \lambda, \epsilon)$ are at most $\mathcal{O}(\epsilon \log(\epsilon))$.

We will first construct an exponential dichotomy on \mathbb{R}^\pm for the singular system

$$z' = A(\xi, \lambda, 0)z, \quad (6.2)$$

for all values of $\lambda \in \Omega$ with constants $K^0(\lambda)$, $L^0(\lambda)$, $\alpha^0(\lambda)$ and $\beta^0(\lambda)$. We will then show that these exponential dichotomies persist for the flow of the full system with constants $K(\lambda)$, $L(\lambda)$, $\alpha(\lambda)$ and $\beta(\lambda)$,

albeit only on the asymptotically large interval J_f . A key point will be to show that these constants can be defined to be $\mathcal{O}(1)$ in ϵ . Finally, we will show that these constants may also be chosen independent of $\lambda \in \Omega$. This will imply the existence of an exponential dichotomy on J_f with projection $Q_f(\xi, \lambda, \epsilon)$ and constants,

$$K_f = \sup_{\lambda \in \Omega} K(\lambda), \quad L_f = \sup_{\lambda \in \Omega} L(\lambda), \quad \alpha_f = \inf_{\lambda \in \Omega} \beta(\lambda), \quad \beta_f = \inf_{\lambda \in \Omega} \beta(\lambda).$$

To begin, the singular system has asymptotic limits,

$$A^\pm = \lim_{\xi \rightarrow \pm\infty} A(\xi, \lambda, 0) = \begin{pmatrix} 0 & F & 0 \\ F(f_U(U_\pm, W_f) + \lambda) & cF^2 & FU_\pm \\ 0 & 0 & -\frac{\lambda}{c} \end{pmatrix}.$$

The eigenvalues, $\mu(\lambda)^\pm$, of the asymptotic matrices A^\pm satisfy the condition,

$$\left(-\frac{\lambda}{c} - \mu^\pm\right) \left((\mu^\pm)^2 - cF^2\mu^\pm - F^2(f_U(U_\pm, W_f) + \lambda)\right) = 0.$$

We label the three roots μ_u^\pm , μ_s^\pm and μ_c^\pm and their corresponding eigenvectors v_u^\pm , v_s^\pm and v_c^\pm . Note that $\mu_c^\pm = -\frac{\lambda}{c}$, as in (5.3). For $\text{Re}(\lambda) > 0$, μ_u^\pm is the sole unstable eigenvalue for A^\pm . For $-\delta < \text{Re}(\lambda) < 0$, μ_c^\pm is also unstable. There is no problem, so long as a spectral gap exists between μ_c^\pm and μ_u^\pm . Both asymptotic limits for the singular problem correspond to points on a stable branch of the slow manifold wherein we have $f_U > 0$. In particular, $f_U(U_\pm, W_f) > ka$ for the front. Therefore, $\mu_u^\pm(\lambda) > cF^2(0) > \mu_s^\pm(\lambda)$, whenever $\delta < ka$. We must simply verify that $\frac{\delta}{c} < cF^2(0)$. This follows since,

$$\delta < \frac{k}{24}(1+a)^2 < \frac{16k}{24} \left(\frac{F(W_b)}{F(0)}\right)^2 \left(\frac{1}{2} - a\right)^2 < (cF(W_b))^2 < (cF(0))^2, \quad (6.3)$$

where the first inequality follows from our assumptions on Ω and the second follows from the assumption that the critical wavespeed for the back is less than the wavespeed selected by the front. In this way, the asymptotic eigenvalues have a spectral gap between the unstable and weakly-unstable eigenvalues for all $\xi \in J_f$ when $-\delta < \text{Re}(\lambda) < 0$.

Note that $A(\xi, \lambda, 0)$ has an invariant subspace given by $r = 0$. Let $y = (p, q)^T$ and consider the reduced system restricted to this subspace,

$$y' = A_R(\xi, \lambda)y.$$

Values of λ for which there exist bounded solutions on \mathbb{R} to this equation correspond to spectral values of the linearized operator \mathcal{L}^f along the front, recall the definition in Section 5.2. We have that $\sigma(\mathcal{L}^f) \cap \Omega$ at the single point $\lambda = 0$. This implies that the reduced system has an exponential dichotomy on both half lines, \mathbb{R}^+ and \mathbb{R}^- , for all $\lambda \in \Omega$. Let $P_R^\pm(\xi, \lambda) : \mathbb{R} \times \mathbb{C}^2 \rightarrow \mathbb{C}^2$ be the projection operator for the reduced system associated to the exponential dichotomies. For all $\lambda \neq 0$, we may choose $P_R^+(0, \lambda) = P_R^-(0, \lambda)$. We will show that (6.2) also has this property.

Lemma 6.1. *For each $\lambda \in \Omega$, the linear system (6.2) has an exponential dichotomy on \mathbb{R}^\pm with constants $K^0(\lambda)$, $L^0(\lambda)$, stable decay rate $\alpha^0 < \min_{\lambda \in \Omega} \{ \text{Re} \frac{\lambda}{c}, -\text{Re} \mu_s^\pm(\lambda) \}$, unstable decay rate $\beta^0(\lambda) = \inf_{\lambda \in \Omega} \{ \text{Re} \mu_u^\pm(\lambda) \}$, and analytic projections $P_f^\pm(\xi, \lambda)$ satisfying $P_f^+(\xi, \lambda) = P_f^-(\xi, \lambda)$ for all $\lambda \neq 0$. Finally, we have $|P_f^+(\xi_r, \lambda) - P_\infty^+(\lambda)| = \mathcal{O}(\epsilon)$ where $P_\infty^+(\lambda)$ is the stable spectral projection for the asymptotic system A^+ .*

Proof: We consider the case of \mathbb{R}^+ , the situation for \mathbb{R}^- is similar. Choose α^0 so that

$$\max_{\lambda \in \Omega} \{ \text{Re}(\mu_c(\lambda)), \text{Re}(\mu_s^\pm(\lambda)) \} < -\alpha^0 < \min_{\lambda \in \Omega} \text{Re}(\mu_u^\pm(\lambda)).$$

By the estimates in (6.3) such a choice is possible. Let $P_\infty^+(\lambda)$ be the spectral projection associated to the eigenvalues μ_c^+ and μ_s^+ . It is clear that $x' = A^+(\lambda)x$ has an exponential dichotomy on \mathbb{R}^+ for any value of $\lambda \in \Omega$ (allowing $\alpha < 0$ if necessary). We note that the constants $K^0(\lambda)$ and $L^0(\lambda)$ are continuous with respect to λ . This is observed since

$$e^{tA^+(\lambda)} P_+^\infty = \frac{1}{2\pi i} \int_\gamma (A^+(\lambda) - zI)^{-1} e^{tz} dz,$$

where γ is a closed curve in \mathbb{C} surrounding $\mu_c^+(\lambda)$ and $\mu_s^+(\lambda)$ for all $\lambda \in \Omega$, with maximal real part $-\alpha^0$ so that it does not enclose any $\mu_u^+(\lambda)$. Then

$$|e^{tA^+(\lambda)} P_+^\infty| \leq \frac{1}{2\pi} \int_\gamma |(A^+(\lambda) - zI)^{-1}| |dz| e^{-\alpha^0 t},$$

so that

$$K^0(\lambda) = \frac{1}{2\pi} \int_\gamma |(A^+(\lambda) - zI)^{-1}| |dz|,$$

and is continuous in λ . Let $C(\xi, \lambda) = A(\xi, \lambda, 0) - A^+(\lambda)$. Then $|C(\xi, \lambda)| \leq C_f e^{-d\xi}$ as $\xi \rightarrow \infty$ for some $d > 0$ and Theorem 8 implies that (6.2) has an exponential dichotomy on \mathbb{R}^\pm with the same decay rates as the limiting system, A^+ . This establishes the first part of the lemma, for the remainder we appeal to the mechanics of the proof of Theorem 8.

Without loss of generality, assume that the stable and unstable decay rates are equal and are $\alpha(\lambda)$. Select ξ_0 so large that $\int_{\xi_0}^\infty |C(\tau, \lambda)| d\tau < 1/(2K^0(\lambda))$. Then the following operator T is a contraction map on the space of continuous, bounded matrix functions of \mathbb{R}^+ ,

$$T\phi(\xi, \xi_0) = e^{A_\infty^+(\xi-\xi_0)} P_\infty^+ + \int_{\xi_0}^\xi e^{A_\infty^+(\xi-\tau)} P_\infty^+ C(\tau, \lambda) \phi(\tau, \xi_0) d\tau - \int_\xi^\infty e^{A_\infty^+(\xi-\tau)} (1 - P_\infty^+) C(\tau, \lambda) \phi(\tau, \xi_0) d\tau.$$

The unique fixed point, ϕ^* defines the stable projection at ξ_0 , i.e. $P_f^+(\xi_0) = \phi^*(\xi_0, \xi_0)$. The projection at other values of ξ can be found using the flow property, see (4.4). This leads to the following equality,

$$\begin{aligned} P_f^+(\xi, \lambda) - P_\infty^+(\lambda) &= - \int_{\xi_0}^\xi e^{A_\infty^+(\xi-\tau)} P_\infty^+(\lambda) C(\tau, \lambda) X(\tau, \xi) (1 - P_f^+(\xi, \lambda)) d\tau \\ &\quad - \int_\xi^\infty e^{A_\infty^+(\xi-\tau)} (1 - P_\infty^+) C(\tau, \lambda) X(\tau, \xi) P_f^+(\xi, \lambda) d\tau. \end{aligned}$$

Here $X(\xi, \xi_0)$ is the fundamental matrix solution for (6.2). Since $\xi_r = -\theta_f \log(\epsilon)$, for θ_f arbitrary but $\mathcal{O}(1)$, we may select θ_f so that $|P_f^+(\xi_r, \lambda) - P_\infty^+(\lambda)| = \mathcal{O}(\epsilon)$ holds. Note that the spectral projection P_∞^+ depends analytically on λ . The projection $P_f^\pm(\xi, \lambda)$ is also analytic since it is given as the limit of analytic functions that converge uniformly on Ω .

The range of $P_f(\xi, \lambda)$ is unique, but its nullspace is not. By the above construction, we have $\ker P_f(\xi_0, \lambda) = \ker P_\infty^+(\lambda)$. The same analysis applies if we were to start with a different projection $P_\infty^{new}(\xi, \lambda)$ for the asymptotic system, A^+ . In particular, we still have $|P_f^+(\xi_r, \lambda) - P_\infty^+(\lambda)| = \mathcal{O}(\epsilon)$ since $|P_f^+(\xi_r, \lambda) - P_\infty^{new}(\xi_r, \lambda)|$ behaves as before and $|P_\infty^{new}(\xi, \lambda) - P_\infty^+(\lambda)|$ goes to zero exponentially as $\xi \rightarrow \infty$.

We now consider all of \mathbb{R} . The subspace $r = 0$ is invariant and an exponential dichotomy exists there on \mathbb{R}^\pm . It only remains to show that the final direction can be chosen appropriately. This follows since the stable projection on the positive half-line is unique and must have component in the r direction. Thus, there is a stable projection on \mathbb{R}^\pm and it is given by

$$P_f^\pm(\xi, \lambda) = \begin{pmatrix} P_R^\pm(\xi, \lambda) & v(\xi, \lambda) \\ 0 & 1 \end{pmatrix}. \quad (6.4)$$

The matrix is written in block form, so v is a two dimensional vector. Finally, for all $\lambda \in \Omega$, $\lambda \neq 0$, we may select $P_f^+(\lambda) = P_f^-(\lambda)$ and an exponential dichotomy then exists on all of \mathbb{R} with the appropriate modifications of the unstable and stable decay rates. ■

We now analyze the full problem (6.1) over the front for sufficiently small ϵ . Divide the interval J_f into two pieces:

$$J_f^- := (-\infty, 0), \quad J_f^+ := (0, -\theta_f \log(\epsilon)).$$

Lemma 6.2. *For all $(k, a, c_1, M) \in \Pi$, there exists an $\epsilon_f > 0$ such that for all $0 < \epsilon < \epsilon_f$ and $\lambda \in \Omega$, the equation (6.1) has an exponential dichotomy on \mathbb{R}^\pm with analytic stable projections $Q_f^\pm(\xi, \lambda, \epsilon)$ and constants $K(\lambda)$, $L(\lambda)$, $\alpha(\lambda)$ and $\beta(\lambda)$. Furthermore, K and L are $\mathcal{O}(1)$ with respect to ϵ , $\beta(\lambda) = \beta^0(\lambda) + \mathcal{O}(\epsilon \log(\epsilon))$, $\alpha(\lambda) = \alpha^0(\lambda) + \mathcal{O}(\epsilon \log(\epsilon))$ and $Q_f^\pm(\xi, \lambda, \epsilon) = P_f^\pm(\xi, \lambda) + \mathcal{O}(\epsilon \log(\epsilon))$.*

Proof: The existence of the exponential dichotomy follows from standard roughness of dichotomy results, see Theorem 7. The one subtlety is the fact that for ϵ small but non-zero, the interval J_f^+ is finite, so exponential dichotomies exist there trivially for any choice of the projection. To avoid this problem, we expand J_f^+ to all of \mathbb{R}^+ in such a way that $|B(\xi, \lambda, \epsilon)| = \mathcal{O}(\epsilon \log(\epsilon))$ for all $\xi \in \mathbb{R}^+$. Following the proof of Proposition 4.1 in [6], the unique bounded matrix solution to the full problem is given as the fixed point of the following integral equation,

$$\begin{aligned} T\phi(\xi) = X(\xi, \xi_0)P_f^+(\xi_0, \lambda) &+ \int_{\xi_0}^{\xi} X(\xi, s)P_f^+(s, \lambda)B(s)\phi(s)ds \\ &- \int_{\xi}^{\infty} X(\xi, s)(1 - P_f^+(s, \lambda))B(s)\phi(s)ds. \end{aligned}$$

It is easy to show that this constitutes a contraction mapping on the space of uniformly continuous, bounded matrix functions on \mathbb{R}^+ with contraction constant $\theta = \mathcal{O}(\epsilon \log(\epsilon))$. The unique fixed point of the mapping is given by $\phi^*(s)$. The stable projection for the perturbed system is then given by $Q_f^+(\xi_0, \lambda, \epsilon) = \phi^*(\xi_0)$ and the estimate $Q_f^\pm(\xi, \lambda, \epsilon) = P_f^\pm(\xi, \lambda) + \mathcal{O}(\epsilon \log(\epsilon))$ follows from [6]. When restricted to J_f , the projection is not unique. However, any two different projections differ by only $\mathcal{O}(\epsilon^{1+\theta_f\beta^0} \log(\epsilon))$ amounts. If the extension to all of \mathbb{R}^+ was done so that $B(\xi, \lambda, \epsilon)$ is analytic in λ for all $\xi \in \mathbb{R}^+$ then the projection $Q_f^+(\xi, \lambda, \epsilon)$ is analytic as well. In addition, we have (see Proposition 4.1 in [6])

$$\begin{aligned} L(\lambda) &= \frac{2(L^0)^2}{1 + 2L^0 + (1 + 2L^0)\sqrt{1 - 2\theta} - 4L^0} \quad , \quad K(\lambda) = \frac{2(K^0)^2}{1 + 2K^0 + (1 + 2K^0)\sqrt{1 - 2\theta} - 4K^0} \\ \beta(\lambda) &= \beta^0\sqrt{1 - 2\theta} \quad , \quad \alpha(\lambda) = \alpha^0\sqrt{1 - 2\theta}, \end{aligned}$$

where we see that $K(\lambda)$ and $L(\lambda)$ are both $\mathcal{O}(1)$ and $\beta(\lambda) = \beta^0 + \mathcal{O}(\epsilon \log(\epsilon))$ and $\alpha(\lambda) = \alpha^0 + \mathcal{O}(\epsilon \log(\epsilon))$. ■

This establishes uniformity of the exponential dichotomies with respect to ϵ . To show the same for λ , we will need to define new constants

$$K_f = L_f = \sup_{\lambda \in \Omega} L(\lambda), \quad \beta_f = \inf_{\lambda \in \Omega} \beta(\lambda), \quad \alpha_f = \inf_{\lambda \in \Omega} \alpha(\lambda).$$

The α_f and β_f are $\mathcal{O}(\epsilon \log(\epsilon))$ close to $\alpha^0(\lambda)$ and $\beta^0(\lambda)$. In turn, these attain their minimum on the boundary of Ω , at $\lambda = -\delta$. Since there is a spectral gap at this point, there remains a spectral gap between α_f and β_f for sufficiently small values of ϵ .

To recap, we have shown that there exists $Q_f^\pm(\xi, \epsilon, \lambda)$, K_f , L_f , α_f and β_f so that

$$\begin{aligned} |X(\xi_2, \xi_1)Q_f^\pm(\xi_1, \epsilon, \lambda)| &\leq K_f e^{-\alpha_f(\xi_2 - \xi_1)} \quad \text{for } \xi_2 \geq \xi_1 \quad \xi_1, \xi_2 \in J_f^\pm \\ |X(\xi_2, \xi_1)(1 - Q_f^\pm(\xi_1, \epsilon, \lambda))| &\leq L_f e^{-\beta_f(\xi_1 - \xi_2)} \quad \text{for } \xi_1 \geq \xi_2 \quad \xi_1, \xi_2 \in J_f^\pm. \end{aligned}$$

This has been shown along the front. We conclude the analysis of the front with an important observation.

Corollary 1. *The subspace of solutions for the full system that converge to the origin as $\xi \rightarrow -\infty$ is given exactly by the range of Q_f^- . In other words,*

$$P^-(0, \lambda, \epsilon) = Q_f^-(0, \lambda, \epsilon).$$

6.2 The Back

To construct an exponential dichotomy for the solution of the eigenvalue problem along the back we would like to follow the same approach as that of the front. In that situation, the exponential decay of the leading order solution to the rest points along the slow manifold allowed for the construction of a leading order exponential dichotomy with decay rates specified by the exponential behavior of the rest state. A perturbation argument was then used to extend this dichotomy to the full system, albeit on a smaller, asymptotically large domain in ξ . We will use the same general approach for the back, however, the algebraic instead of exponential decay of the solution to the knee will complicate the analysis considerably.

We begin the analysis of the back by introducing a new variable, χ . We will select $\chi = 0$ to correspond to the unique point along the back where $U = \frac{(1+a)}{3}$. In this way, the interval $J_b = (\xi_b(\epsilon), \xi_l(\epsilon))$ in ξ corresponds to an interval in χ of the form $(-\frac{\theta_k}{\epsilon^{1/3}}, -\theta_l \log(\epsilon))$. In terms of this new variable, we have that

$$\begin{aligned} U(\chi) &= U_b(\chi) + \epsilon^{1/3}U_1(\chi, \epsilon) \\ W(\chi) &= W_b + \epsilon^{1/3}W_1(\chi, \epsilon), \end{aligned}$$

with $|U_1|$ and $|W_1|$ bounded by a constant M_b , independent of ϵ . As we did for the front, our approach will consist of three steps. First, we consider the reduced ($w = W_b$), singular ($\epsilon = 0$) case and show that this system has an exponential dichotomy for all $\lambda \in \Omega$. Second, we extend this exponential dichotomy in the singular case to all three dimensions. Finally, we show that this solution persists using Theorem 7.

Following subsection 6.1 we write the linearized eigenvalue problem as

$$x' = (A(\chi, \lambda, 0) + B(\chi, \lambda, \epsilon))x, \quad (6.5)$$

for $x = (p, q, r)^T$. The singular system is given by

$$A(\chi, \lambda, 0) = \begin{pmatrix} 0 & F & 0 \\ F(f_U(U_b, W_b) + \lambda) & cF^2 & Ff_W(U_b, W_b) + 2\frac{F_W}{F^2}U_b'' - \frac{\lambda}{cF^2}F_WU_b' \\ 0 & 0 & -\frac{\lambda}{c} \end{pmatrix}.$$

Let $A^\pm = \lim_{\chi \rightarrow \pm\infty} A(\chi, \lambda, 0)$. As was the case with the front, the $r = 0$ subspace is invariant under the singular flow. The dynamics in this invariant subspace is given by the system $y' = A_R(\chi, \lambda)y$ with

$$A_R(\chi, \lambda) = \begin{pmatrix} 0 & F(W_b) \\ F(W_b)(f_U(U_b, W_b) + \lambda) & cF(W_b)^2 \end{pmatrix}.$$

This system is precisely the linearized eigenvalue problem associated to the Fisher-type equation for the jump back. The spectrum of this systems has been studied in [37], the results of which are summarized in the following lemma.

Lemma 6.3. *Fix $(k, a, M, c_1) \in \Pi$. For all $\lambda \in \Omega$, the system $y' = A_R(\chi, \lambda)y$ has an exponential dichotomy on \mathbb{R} with projection $P_R^b(\chi, \lambda)$.*

Proof: The proof follows the one contained in [37], where n-degree Fisher equations were studied. It can be summarized as follows. The existence of a spectral gap between the limiting eigenvalues is shown. The slow algebraic decay prevents the direct application of Theorem 8, since $A(\chi, \lambda, 0) - A^-$ is not integrable. The existence of a spectral gap for all $\chi < 0$ allows for a diagonalization of the leading order system. This system can be solved by exponentiation and the decay rates can be bounded in this way. The next order correction now involves derivatives of the linearizing transformation and therefore it converges with at least rate $\mathcal{O}(C/\chi^2)$ and Theorem 8 can now be applied. This establishes an exponential dichotomy and then Sturm-Liouville arguments can be applied to show that this exponential dichotomy may always be extended to all of \mathbb{R} (i.e there exists $D_B(\lambda) \neq 0$).

We must show that the same technique may be applied consistently for all parameter values in Π , that is, we must demonstrate the existence of a spectral gap between the frozen eigenvalues so that the diagonalization step is justified. The remainder of the proof follows as in [37]. Recall that at the knee $(U, W) = (u_{knee}, w_{knee})$, we have $f_U(u_{knee}, w_{knee}) = 0$. In addition, we have that $f_U(U_b, W_b) < 0$ close to the knee. Near the left most

side of Ω we must ensure that a spectral gap exists between μ_u and μ_s (a gap between μ_u and μ_c was shown in (6.3)). In other words, we must show that the $\text{Re}(c^2 F(W_b)^4 + 4F(W_b)^2(f_U(U_b, W_b) + \lambda)) > 0$. Any easy calculation finds that $f_U(U_b, W_b)$ attains its minima at $U_{min} = \frac{1}{3}(1+a)$ and that $f_U(U_{min}, W_b) = \frac{-k}{12}(1+a)$. Then,

$$\begin{aligned} c^2 F(W_b)^4 + 4F(W_b)^2 f_U(U_{min}, W_b) &= F(W_b)^2 \left(\frac{2k(1+a)^2 F(W_b)^2}{F(0)^2} - \frac{k(1+a)^2}{3} \right) \\ &= k(1+a)^2 F(W_b)^2 \left(\frac{2F(W_b)^2}{F(0)^2} - \frac{1}{3} \right) \geq \frac{k(1+a)^2 F(W_b)^2}{6} \end{aligned} \quad (6.6)$$

The last inequality follows since $2F(W_b) > F(0)$ for parameters in Π . Then, selecting $0 < \delta < \frac{k(1+a)^2}{24}$ implies that $\text{Re}(\mu_u(\xi, \lambda)) > \text{Re}(\mu_s(\xi, \lambda))$ for ξ along the back and $\lambda \in \Omega$. Due to this spectral gap, there exists a diagonalizing transformation $Q(\chi, \lambda)$, and the proof in [37] can be extended. ■

We do not remark on the analyticity of the projection P_R^b , although it is also studied in [37]. This is because we will only use the projection along the back as a skeleton by which to track the analytic projection $P^+(0, \lambda, \epsilon)$ and this process will not require analyticity of P_R^b . Next, we extend these exponential dichotomies to all of \mathbb{C}^3 .

Lemma 6.4. *Fix $(k, a, M, c_1) \in \Pi$. For all $\lambda \in \Omega$, the singular problem $z' = A(\chi, \lambda, 0)z$ has an exponential dichotomy on \mathbb{R} with projections $P_b(\chi, \lambda)$ and constants $K_b^0(\lambda)$, $L_b^0(\lambda)$, $\alpha_b^0(\lambda)$ and $\beta_b^0(\lambda)$. In addition, we have $|P_b(\xi_b, \lambda) - P_{knee}(\lambda)| = \mathcal{O}(\epsilon^{1/3})$ and $|P_b(\xi_l, \lambda) - P_{b,\infty}^+(\lambda)| = \mathcal{O}(\epsilon)$ where $P_{knee}(\lambda)$ is the spectral projection associated to stable eigenvalues of A^- and $P_{b,\infty}^+(\lambda)$ is the same for A^+ .*

Proof: We proceed as we did for the front. The exponential convergence of $A(\chi, \lambda, 0)$ to its asymptotic state as $\chi \rightarrow \infty$ implies that the analysis will be identical to that of the front for \mathbb{R}^+ . Thus, we consider $\chi < 0$. Due to the slow convergence of $A(\chi, \lambda, 0)$ to its asymptotic state as $\chi \rightarrow -\infty$, it is again not possible to apply Theorem 8 and find an exponential dichotomy with the same decay rates as A^- . However, we recall that the spectral gap between unstable and weakly unstable eigenvalues persists for the full system due to the calculation in (6.3). This gives the existence of α_b^0 and β_b^0 such that

$$\max_{\lambda \in \Omega} \{\text{Re}(\mu_c(\lambda)), \text{Re}(\mu_s(\chi, \lambda))\} < -\alpha_b^0 < \beta_b^0 < \min_{\lambda \in \Omega} \text{Re}(\mu_u(\chi, \lambda)).$$

Let $C(\chi, \lambda) = A(\chi, \lambda, 0) - A^-$. To show the existence of an exponential dichotomy, we set up a fixed point equation as we did before,

$$\begin{aligned} T\phi(\chi, \chi_0) &= e^{A^-(\chi-\chi_0)}(1 - P_{knee}) - \int_{\chi}^{\chi_0} e^{A^-(\chi-\tau)}(1 - P_{knee})C(\tau, \lambda)\phi(\tau, \chi_0)d\tau \\ &+ \int_{-\infty}^{\chi} e^{A^-(\chi-\tau)}P_{knee}C(\tau, \lambda)\phi(\tau, \chi_0)d\tau. \end{aligned}$$

We can not apply Theorem 8 ($C(\chi)$ is not integrable). Instead we fix $\chi_0 < 0$ large enough so that we may apply Theorem 7 to conclude the existence of an exponential dichotomy with decay rates α_b^0 and β_b^0 (see also [31] for a similar argument using Fredholm properties). The unique fixed point of the operator, T_ϕ , when

evaluated at $\chi = \chi_0$ is the unstable projection $(1 - P_b(\chi_0, \lambda))$. Now we have,

$$\begin{aligned}
(1 - P_b(\chi, \lambda)) &= X(\chi, \chi_0)(1 - P_b(\chi_0, \lambda))X(\chi_0, \chi) = \phi^*(\chi, \chi_0)X(\chi_0, \chi) \\
&= e^{A^-(\chi - \chi_0)}(1 - P_{knee})X(\chi_0, \chi) - \int_{\chi}^{\chi_0} e^{A^-(\chi - \tau)}(1 - P_{knee})C(\tau, \lambda)\phi^*(\tau, \chi_0)X(\chi_0, \chi)d\tau \\
&+ \int_{-\infty}^{\chi} e^{A^-(\chi - \tau)}P_{knee}C(\tau, \lambda)\phi^*(\tau, \chi_0)X(\chi_0, \chi)d\tau \\
&= (1 - P_{knee}) + \int_{\chi}^{\chi_0} e^{A^-(\chi - \tau)}(1 - P_{knee})C(\tau, \lambda)X(\tau, \chi)d\tau \\
&- \int_{\chi}^{\chi_0} e^{A^-(\chi - \tau)}(1 - P_{knee})C(\tau, \lambda)\phi^*(\tau, \chi_0)X(\chi_0, \chi)d\tau \\
&+ \int_{-\infty}^{\chi} e^{A^-(\chi - \tau)}P_{knee}C(\tau, \lambda)\phi^*(\tau, \chi_0)X(\chi_0, \chi)d\tau \\
&= (1 - P_{knee}) + \int_{\chi}^{\chi_0} e^{A^-(\chi - \tau)}(1 - P_{knee})C(\tau, \lambda)X(\tau, \chi)P_b(\chi, \lambda)d\tau \\
&+ \int_{-\infty}^{\chi} e^{A^-(\chi - \tau)}P_{knee}C(\tau, \lambda)X(\tau, \chi)(1 - P_b(\chi, \lambda))d\tau.
\end{aligned}$$

The algebraic decay of the solution to its asymptotic limit implies that there exists a $K_c > 0$ so that for all $\tau < \chi_0$ we have $|C(\tau, \lambda)| \leq -\frac{K_c}{\tau}$. Then,

$$\begin{aligned}
|P_b(\chi, \lambda) - P_{knee}(\lambda)| &\leq K^0 K K_c \int_{\chi}^{\chi_0} \frac{e^{-(\beta_b^0 + \alpha_b^0)(\tau - \chi)}}{-\tau} d\tau + L^0 L K_c \int_{-\infty}^{\chi} \frac{e^{-(\alpha_b^0 + \beta_b^0)(\chi - \tau)}}{-\tau} d\tau \\
&\leq \frac{\tilde{K}}{(\beta_b^0 + \alpha_b^0)|\chi|} + \tilde{K} e^{(\beta_b^0 + \alpha_b^0)\chi} \int_{\chi}^{\chi_0} \frac{e^{-(\beta_b^0 + \alpha_b^0)\tau}}{(\beta_b^0 + \alpha_b^0)\tau^2} d\tau + \frac{\tilde{L}}{(\alpha_b^0 + \beta_b^0)|\chi|},
\end{aligned}$$

where we have integrated by parts and neglected negative terms in the first integral. Since χ_0 is fixed, we have for $\chi < 0$ and sufficiently large, the second integral is dominated by its value at χ . This leads to the following characterization,

$$|P_b(\chi, \lambda) - P_{knee}(\lambda)| = \mathcal{O}(|\chi|^{-1}) \quad \text{as } \chi \rightarrow -\infty.$$

Since, $\chi_k = -\theta_k \epsilon^{-1/3}$, this implies that $|P_b(\chi_k, \lambda) - P_{knee}(\lambda)| = \mathcal{O}(\epsilon^{1/3})$ as required. As was the case with the front, changing the range of $(1 - P_b(\chi, \lambda))$ (the nullspace of $P_b(\chi, \lambda)$) does not affect the results. ■

This leads to the following result.

Lemma 6.5. *For all $\lambda \in \Omega$ and ϵ sufficiently small, the system (6.5) has an exponential dichotomy on J_b with projection $Q_b(\xi, \lambda, \epsilon)$ and constants $K_b, L_b, \alpha_b,$ and β_b . Furthermore, we have that*

$$|Q_b(\xi_b, \lambda, \epsilon) - Q_k(\xi_b, \lambda, \epsilon)| = \mathcal{O}(\epsilon^{1/3}).$$

Proof: The persistence of the dichotomy for small $\epsilon \neq 0$ is a consequence of the roughness of exponential dichotomies as in the case of the front, see Theorem 7. ■

6.3 The Right Slow Manifold

In this section, we will show the existence of an exponential dichotomy for the solution of the linearized eigenvalue for all $\xi \in J_r$ and ϵ sufficiently small. We have the following result,

Lemma 6.6. For all $(k, a, c_1, M) \in \Pi$ there exists an ϵ_r such that for all $0 < \epsilon < \epsilon_r$ the linearized eigenvalue problem $x' = A(\xi, \lambda, \epsilon)x$ has an exponential dichotomy on J_r with projection $Q_r(\xi, \lambda, \epsilon)$ and constants, $K_r, L_r, \alpha_r < \inf_{\xi \in J_r, \lambda \in \Omega} \min\{\operatorname{Re}(-\mu_s(\xi, \lambda)), \operatorname{Re} \frac{-\lambda}{c}\}$ and $\beta_r < \inf_{\xi \in J_r, \lambda \in \Omega} \operatorname{Re} \mu_u(\xi, \lambda)$, all defined $\mathcal{O}(1)$ with respect to ϵ . If $P_r(\xi, \lambda)$ is the spectral projection for $A(\xi, \lambda, \epsilon)$ for each $\xi \in J_r$, then we have $|Q_r(\xi, \lambda, \epsilon) - P_r(\xi, \lambda)| = \mathcal{O}(\epsilon)$ for all $\xi \in J_r$.

Proof: Along the slow manifold, the linearized eigenvalue problem varies slowly with ξ . The existence of an exponential dichotomy with the above properties is a direct result of Theorem 9, see Proposition 6.1 in [6]. ■

We conclude with a result that compares the projections at the transition point between the front and the right slow manifold.

Lemma 6.7. For all $\lambda \in \Omega$ and ϵ sufficiently small, we have,

$$|Q_f(\xi_r, \lambda, \epsilon) - Q_r(\xi_r, \lambda, \epsilon)| = \mathcal{O}(\epsilon \log(\epsilon)). \quad (6.7)$$

Proof: From Lemma 6.1, Lemma 6.2 and Lemma 6.6,

$$\begin{aligned} |P_f^+(\xi_r, \lambda) - P_\infty^+(\lambda)| &= \mathcal{O}(\epsilon) \\ |Q_f(\xi_r, \lambda, \epsilon) - P_f^+(\xi_r, \lambda)| &= \mathcal{O}(\epsilon \log(\epsilon)) \\ |Q_r(\xi_r, \lambda, \epsilon) - P_r(\xi_r, \lambda)| &= \mathcal{O}(\epsilon). \end{aligned}$$

Note that $P_r(\xi_r, \lambda) = P_\infty^+(\lambda)$ since both are the spectral projection of the linearized eigenvalue problem at $\epsilon = 0$ and $(U, W) = (1, 0)$. The result follows. ■

6.4 The Left Slow Manifold

The analysis along the left slow manifold is similar to that of the right slow manifold. Therefore, we have

Lemma 6.8. For all $\lambda \in \Omega$ and ϵ sufficiently small, the linearized eigenvalue problem on $(\xi_l(\epsilon), \infty)$ has an exponential dichotomy with analytic projection $Q_l(\xi, \lambda, \epsilon)$ and constants K_l, L_l, α_l and β_l . In addition, we have that the range of $Q_l(\xi, \lambda, \epsilon)$ describes the unique space of solutions that tend to zero as $\xi \rightarrow \infty$, i.e. $Q_l(\xi, \lambda, \epsilon) = P^+(\xi, \lambda, \epsilon)$. Also, we have

$$|Q_l(\xi_l, \lambda, \epsilon) - Q_b(\xi_l, \lambda, \epsilon)| = \mathcal{O}(\epsilon \log(\epsilon)).$$

Proof: The proof is analogous to the right slow manifold. The one additional detail is to justify that $Q_l(\xi, \lambda, \epsilon)$ is analytic, which follows due to the analyticity of the spectral projections and arguments similar to those used to show analyticity for the front. ■

6.5 The Knee

In subsection B.2, the flow as it passes the knee is broken into three pieces corresponding to the various charts introduced in [23]. The interval $(\xi_k(\epsilon), \xi_b(\epsilon))$ corresponds to the solution as it traverses from Σ_2^{in} to Σ_2^{out} in chart K_2 . For the purposes of this subsection, it is only important that while in the chart K_2 , the solution can be represented as

$$(u, w) = (u_{knee}, w_{knee}) + \mathcal{O}(\epsilon^{1/3}),$$

where u_{knee} and w_{knee} are the coordinates of the knee. This allows us to write the linearized eigenvalue problem near the knee as

$$x' = (A_{knee}(\lambda) + B(\xi, \lambda, \epsilon))x, \quad (6.8)$$

where $\sup_{\xi \in J_k} |B| \leq C_k \epsilon^{1/3}$ and,

$$A_{knee}(\lambda) = \begin{pmatrix} 0 & F(w_{knee}) & 0 \\ F(w_{knee})\lambda & cF(w_{knee})^2 & F(w_{knee})u_{knee} \\ 0 & 0 & -\frac{\lambda}{c} \end{pmatrix}.$$

We will attain the following result.

Lemma 6.9. *For all $\lambda \in \Omega$, and for ϵ sufficiently small, the system (6.8) has an exponential dichotomy with projection $Q_k(\xi, \lambda, \epsilon)$ and constants K_k, L_k, α_k and β_k . Furthermore, we have*

$$|Q_r(\xi_k, \lambda, \epsilon) - Q_k(\xi_k, \lambda, \epsilon)| = \mathcal{O}(\epsilon^{1/3}).$$

Proof: The proof follows from Theorem 7. The leading order system has an exponential dichotomy since it is constant coefficient. The techniques involved are very similar to the case of the front so we will not repeat them here. ■

6.6 Tracking the subspaces $P^+(0, \lambda, \epsilon)$ and $1 - P^-(0, \lambda, \epsilon)$

Eigenvalues in Ω are given by values of λ for which the stable subspace at $\xi = \infty$ intersects nontrivially with the unstable subspace at $\xi = -\infty$. In the preceding analysis, these subspaces were constructed as $Q_l(\xi, \lambda, \epsilon)$ and $1 - Q_f(\xi, \lambda, \epsilon)$ respectively. In order to locate eigenvalues, we must compare the subspaces at the same value of ξ . Therefore, it will be necessary to track these subspaces as they evolve along the wave. We will use the exponential dichotomies constructed in the previous sections to accomplish this. The essential elements that we must understand are how subspaces evolve under exponential dichotomies and how to transform these subspaces and we pass from one exponential dichotomy to the next. The following lemma will be instrumental in this analysis. It is reminiscent of the elephant trunk lemma [13].

Lemma 6.10. *Suppose that the system $x' = A(\xi, \epsilon, \lambda)x$ has an exponential dichotomy on the interval $(a_1(\epsilon), a_2(\epsilon)]$ with projection $Q_1(\xi, \epsilon)$ and constants K_1 and α_1 on the unstable subspace and L_1 and β_1 for the stable subspace. Likewise, suppose that on the interval $[a_2(\epsilon), a_3(\epsilon))$ the system also has an exponential dichotomy with projection $Q_2(\xi, \epsilon)$ and constants K_2, α_2, L_2 and β_2 . Suppose that at the transition point, $|Q_1(a_2, \epsilon) - Q_2(a_2, \epsilon)| < \gamma$, for a sufficiently small value of γ .*

Let $0 < \mu < 1$ and consider $v \in \mathbb{C}^3$ so that

$$\frac{|Q_1(a_1, \epsilon)v|}{|(1 - Q_1(a_1, \epsilon))v|} < \mu.$$

Then we have that at $\xi = a_2(\xi, \epsilon)$,

$$\frac{|Q_2 X(a_2, \epsilon)v|}{|(1 - Q_2)X(a_2)v|} \leq \mu_1,$$

with

$$\mu_1 = \frac{2\gamma + \frac{\mu}{K_1 L_1} e^{-(\alpha_1 + \beta_1)\Delta_1(\epsilon)}}{1 - 2\gamma},$$

where $\Delta_1 = a_2(\epsilon) - a_1(\epsilon)$.

Proof: From the definition of exponential dichotomies we find that

$$\frac{|Q_1(a_2)X(a_2, \epsilon)v|}{|(1 - Q_1(a_2))X(a_2)v|} \leq \frac{\mu}{K_1 L_1} e^{-(\alpha_1 + \beta_1)\Delta_1(\epsilon)}.$$

For ease in what follows we will label $\phi_1 = \frac{\mu}{K_1 L_1} e^{-(\alpha_1 + \beta_1)\Delta_1(\epsilon)}$. We suppose that $Q_1 = Q_2 + D$ with $|D| < \gamma$. We then can conclude,

$$\begin{aligned}
|Q_2(a_2)X(a_2)v| &\leq |Q_1(a_2)X(a_2)v| + |DX(a_2)v| \\
&\leq \phi_1|X(a_2)(1 - Q_1(a_1))v| + |D||X(a_2)v| \\
&\leq \phi_1|(1 - Q_2(a_2))X(a_2)v| + 2\gamma|X(a_2)v| \\
&\leq \phi_1|(1 - Q_2(a_2))X(a_2)v| + 2\gamma|Q_2X(a_2)v| + 2\gamma|(1 - Q_2)X(a_2)v|.
\end{aligned}$$

■

Corollary 2. *Under the same hypothesis, we find that if one starts with a cone around the stable direction, then that cone is contracted as we move from $a_3(\xi)$ to $a_2(\xi)$. Then we have at $a_2(\xi)$,*

$$\frac{|(1 - Q_1)X(a_2, \epsilon)v|}{|Q_1X(a_2)v|} \leq \mu_1,$$

where

$$\mu_1 = \frac{2\gamma + \frac{\mu}{K_2L_2}e^{-(\alpha_2+\beta_2)\Delta_2(\epsilon)}}{1 - 2\gamma}.$$

Note that these results still hold even if α_i is negative, provided that the exponential rate β_i is sufficiently large and positive.

6.7 Completion of the Proof of Theorem 3: The Evans Function

We will now use the information derived in subsections 6.1-6.5 to approximate the Evans function for the full problem, (4.2). Recall that $P^+(\xi, \lambda, \epsilon)$ denotes the stable projection for the full linearized eigenvalue problem on \mathbb{R}^+ . Similarly $P^-(\xi, \lambda, \epsilon)$ is the stable projection on the negative half line \mathbb{R}^- . The Evans function can be written as

$$D(\lambda) = \text{rng}P^+(0, \lambda, \epsilon) \wedge \text{rng}(1 - P^-(0, \lambda, \epsilon)).$$

We will establish the following result, which will imply Theorem 3.

Theorem 4. *For all $\lambda \in \Omega$ and $0 < \epsilon < \epsilon_2$ we have*

$$D(\lambda) = D_F(\lambda) + \mathcal{O}(\epsilon \log(\epsilon)).$$

Therefore, $D(\lambda) \neq 0$ in Ω with the exception of a simple zero at the origin.

Proof: To compute the Evans function, we must track $P^+(\xi, \lambda, \epsilon)$ from the interval J_l , wherein we possess an explicit formulation for the projection, to $\xi = 0$ where it will be compared with $P^-(0, \lambda, \epsilon)$. We begin at ξ_l , where

$$P^+(\xi_l, \lambda, \epsilon) = Q_l(\xi_l, \lambda, \epsilon).$$

Fix $0 < \eta_b < 1/3$ and $\mathcal{O}(1)$ in ϵ so that $\eta_b > |Q_l(\xi_l, \lambda, \epsilon) - Q_b(\xi_l, \lambda, \epsilon)| = \mathcal{O}(\epsilon \log(\epsilon))$. This implies that $P^+(\xi_l, \lambda, \epsilon) = Q_b(\xi_l, \lambda, \epsilon) + \mathcal{O}(\epsilon \log(\epsilon))$. Let $v \in \text{rng}P^+(\xi_l, \lambda, \epsilon)$. Then the existence of a spectral gap for the back and the fact that $|J_b| = \mathcal{O}(\epsilon^{-1/3})$ implies by Corollary 2 that

$$|P^+(\xi_b, \lambda, \epsilon) - Q_b(\xi_b, \lambda, \epsilon)| = \mathcal{O}(\epsilon \log(\epsilon)).$$

We now repeat the process. Fix $0 < \eta_k < 1/3$ so that $\eta_k > |Q_b(\xi_b, \lambda, \epsilon) - Q_k(\xi_b, \lambda, \epsilon)| = \mathcal{O}(\epsilon^{1/3})$. Again, there exists a spectral gap and we have that $|J_k| = \mathcal{O}(\epsilon^{-1/3})$. Again Corollary 2 implies that

$$|P^+(\xi_k, \lambda, \epsilon) - Q_k(\xi_k, \lambda, \epsilon)| = \mathcal{O}(\epsilon^{1/3}).$$

Two subsequent applications of this process yield,

$$\begin{aligned}
|P^+(\xi_r, \lambda, \epsilon) - Q_r(\xi_r, \lambda, \epsilon)| &= \mathcal{O}(\epsilon^{1/3}) \\
|P^+(0, \lambda, \epsilon) - Q_f^+(0, \lambda, \epsilon)| &= \mathcal{O}(\epsilon^{1+\alpha_f+\beta_f} \log(\epsilon)).
\end{aligned}$$

Finally, we have by Corollary 1 of Lemma 6.2 that $P^-(0, \lambda, \epsilon) = Q_f^-(0, \lambda, \epsilon)$. Then Lemma 6.2 implies that

$$\begin{aligned} D(\lambda) &= \text{rng} \left(Q_f^+(0, \lambda, \epsilon) + \mathcal{O}(\epsilon \log(\epsilon)) \right) \wedge \text{rng}(1 - Q_f^-(0, \lambda, \epsilon)) \\ &= \text{rng} \left(P_f^+(0, \lambda, \epsilon) \right) \wedge \text{rng} \left(1 - P_f^-(0, \lambda, \epsilon) \right) + \mathcal{O}(\epsilon \log(\epsilon)) \\ &= \text{rng} \left(P_R^+(0, \lambda, \epsilon) \right) \wedge \text{rng} \left(1 - P_R^-(0, \lambda, \epsilon) \right) + \mathcal{O}(\epsilon \log(\epsilon)), \end{aligned}$$

where the last equality follows from (6.4). These projections are analytic in λ and we have that $D(\lambda)$ is asymptotically $\mathcal{O}(\epsilon \log(\epsilon))$ close to $D_F(\lambda)$. Since $D_F(\lambda)$ has only one zero in Ω , then Rouché's Theorem implies that for ϵ sufficiently small $D(\lambda)$ must have only one zero as well. This eigenvalue must lie at the origin due to the translational invariance of the wave. ■

Acknowledgments

The authors thank A. Panfilov for introducing them to this problem and for useful conversations as well as M. Beck for helpful discussions. The research of M.H. was supported by the Center for BioDynamics at Boston University and the NSF (DMS 0602204, EMSW21-RTG) as well as by NSF-DMS 0606343 and NSF-DMS 1004517. The research of T.J.K. was supported by NSF-DMS 0606343 and by NWO. The research of A.D. was supported by NWO.

A Center Manifold Computation

We augment the traveling wave equation with an equation for ϵ . Then the knee,

$$(u, v, w, \epsilon) = (u_{knee}, 0, w_{knee}, 0),$$

is a center-unstable fixed point with one positive eigenvalue and three zero eigenvalues. The positive eigenvalue is $cF^2(w_{knee})$. The corresponding eigenvector is $w_c = \langle 1, cF(w_{knee}), 0, 0 \rangle$. As an eigenvalue, zero has geometric multiplicity one (algebraic multiplicity three), with eigenvector $w_0 = \langle 1, 0, 0, 0 \rangle$ and generalized eigenvector $w_1 = \langle 0, 1, F_W(w_{knee})f(u_{knee}, w_{knee}) + F(w_{knee})u_{knee}, 0 \rangle$, and $w_2 = \langle 0, 0, ku_{knee} - w_{knee}, c(F_W(w_{knee})f(u_{knee}, w_{knee}) + F(w_{knee})u_{knee})^2 \rangle$. For ease of notation, we denote the values of u and w at the knee by

$$\begin{aligned} u_{knee} &= \frac{1+a}{2} \\ w_{knee} &= \frac{k}{4}(1-a)^2. \end{aligned}$$

To compute the center manifold approximation we suppose

$$\begin{aligned} v &= b_{200}(u - u_{knee})^2 + b_{010}(w - w_{knee}) + b_{001}\epsilon + b_{101}\epsilon(u - u_{knee}) + b_{002}\epsilon^2 + b_{020}(w - w_{knee})^2 \\ &+ b_{110}(u - u_{knee})(w - w_{knee}) + b_{011}\epsilon(w - w_{knee}). \end{aligned}$$

In order to proceed, we first expand

$$F(w) = F_0 + F_1(w - w_{knee}) + \dots,$$

where

$$\begin{aligned} F_0 &= \frac{1}{2} \left(1 + \frac{M}{2c_1} \right) + \frac{1}{2} \sqrt{\left(1 + \frac{M}{2c_1} \right)^2 - \frac{2}{c_1} w_{knee}} \\ F_1 &= -\frac{1}{2c_1} \left(\left(1 + \frac{M}{2c_1} \right)^2 - \frac{2}{c_1} w_{knee} \right)^{-1/2}. \end{aligned}$$

The center manifold approximation requires us to express the nonlinearity in terms of local coordinates at the knee,

$$\begin{aligned} ku(u-a)(u-1) + uw &= k(u - u_{knee})^3 + (3ku_{knee} - k(1+a))(u - u_{knee})^2 \\ &+ (u - u_{knee})(w - w_{knee}) + u_{knee}(w - w_{knee}). \end{aligned}$$

The linear terms in $(u - u_{knee})$ drop out since,

$$F_0(3ku_{knee}^2 - 2k(1+a)u_{knee} + ka + w_{knee}) = 0.$$

We now insert the center manifold ansatz into the differential equation for v . Working order by order, the coefficients in the center manifold expansion are computed to be,

$$\begin{aligned} b_{200} &= \frac{k(1+a) - 3ku_{knee}}{cF_0} \\ b_{010} &= \frac{-u_{knee}}{cF_0} \\ b_{001} &= \frac{u_{knee}w_{knee} - ku_{knee}^2}{c^3F_0^3} \end{aligned}$$

The reduced dynamics on the center manifold are then given to leading order by

$$\begin{aligned} u_\xi &= F_0b_{200}(u - u_{knee})^2 + F_0b_{010}(w - w_{knee}) + \dots \\ w_\xi &= \epsilon \left(\frac{ku_{knee}}{c} - \frac{w_{knee}}{c} \right) + \dots \\ \epsilon_\xi &= 0. \end{aligned}$$

B Proof of Lemma 3.4: Corner Estimates

A crucial feature of our approach is the ability to divide the domain, \mathbb{R} into pieces over which the dynamics are effectively described as a perturbation of the front, back, left slow manifold, right slow manifold or near the knee. Within these domains, the solution is either characterized as being pointwise close (in ξ) to the singular solution (front, back, knee) or as evolving at an $\mathcal{O}(\epsilon)$ rate (slow manifolds).

The purpose of this appendix is to explain the tools that we use to justify this decomposition. We review this material in order for the article to be self-contained.

For $\mathcal{O}(1)$ timescales along the front, the true solution remains $\mathcal{O}(\epsilon)$ close to the singular solution. We seek the optimal time scale over which the solution ‘turns a corner’ from evolving pointwise close to the singular solution along the front to evolving at an $\mathcal{O}(\epsilon)$ rate, or equivalently being $\mathcal{O}(\epsilon)$ close to the slow manifold. Hence, the term corner estimates. For entry and exit to the slow manifold at normally hyperbolic points this question has been answered by a theorem in [9]. We state it and repeat the proof here for completeness and for motivation for the case when the exit from the slow manifold does not occur at a normally hyperbolic point.

B.1 Corner estimates - normally hyperbolic points

Before stating the theorem, we note that the theorem relies on the use of Fenichel normal form to describe a neighborhood of the slow manifold. For convenience, we will assume that we are working with the entry to the right slow manifold. The corner estimates for the entry and exit points for the left slow manifold are similar. Here, we assume a transformation has been performed which places the system in Fenichel Normal Form, see [11, 18]. The Fenichel Normal Form is

$$\begin{aligned} a' &= \Lambda(a, b, y, \epsilon)a \\ b' &= \Gamma(a, b, y, \epsilon)b \\ y' &= \epsilon g(a, b, y, \epsilon). \end{aligned}$$

The matrix Λ has spectrum in the right half plane, while the spectrum of Γ lies in the left half plane, with both bounds being strict and independent of ϵ . The slow manifold is represented by the set $(a, b, y) = (0, 0, y)$. Consider a box D surrounding the slow manifold and define two manifolds of entry and exit points,

$$\begin{aligned} N_1 &= \{(a, b, y) \mid a \in [-\Delta, \Delta], b = \Delta, y \in [y_0 - \Delta, y_0 + \Delta]\} \\ N_2 &= \{(a, b, y) \mid a \in [-\Delta, \Delta], b \in [-\Delta, \Delta], y = y_1\}. \end{aligned}$$

We assume for all $\epsilon > 0$ and sufficiently small, there exists a solution entering the slow manifold at time ξ_1 through N_1 and then passing through N_2 at some later time $\xi_2(\epsilon)$, which is $\mathcal{O}(\epsilon^{-1})$. We further assume that this solution satisfies $\lim_{\epsilon \rightarrow 0} y(\xi_1) = y_0$. The dynamics as one enters through N_1 describe the fast layer problem, while as the solution passes through N_2 the leading order the dynamics are given by the slow manifold. We will define a corner function $\Xi(\epsilon)$ that will describe the transition between these two regimes.

Theorem 5. [9] *Let $\Xi(\epsilon)$ satisfy $\lim_{\epsilon \rightarrow 0} \Xi(\epsilon) = \infty$ and $\lim_{\epsilon \rightarrow 0} \epsilon \Xi(\epsilon) = 0$. Then we have that*

$$\lim_{\epsilon \rightarrow 0} (a, b, y)(\Xi(\epsilon), \epsilon) = (0, 0, y_0).$$

Moreover, if $\Xi = -\theta \log(\epsilon)$ for some $\theta > 0$ and if $\|y(\xi_1, \epsilon) - y_0\| = \mathcal{O}(\epsilon)$, then there exists $K > 0$ for which

$$\frac{1}{\epsilon} \|(a, b, y)(\Xi(\epsilon), \epsilon) - (0, 0, y_0)\| \leq K \Xi(\epsilon),$$

as $\epsilon \rightarrow 0$.

Proof: The proof of this theorem can be found in [9]. However, for completeness we will reproduce it here. We will assume that both a and b are one dimensional, which is sufficient for the purposes of this work, but the result is true more generally, see [9]. We assume there exists local constants α_{\pm} and β_{\pm} such that on the box D for sufficiently small ϵ we have,

$$\begin{aligned} 0 < \alpha_- < \Lambda(a, b, y, \epsilon) < \alpha_+ \\ \beta_- < \Gamma(a, b, y, \epsilon) < \beta_+ < 0. \end{aligned}$$

We find that if $\xi > \xi_1$, then

$$|a(\xi)| \geq |a(\xi_1)| e^{\alpha_-(\xi - \xi_1)}.$$

Since $a(\xi_2) \in N_2$, we have

$$|a(\xi_1)| \leq \Delta e^{-\alpha_-(\xi_2 - \xi_1)}.$$

Using the upper bound on Λ , we find in a similar fashion that

$$|a(\Xi(\epsilon))| \leq \Delta e^{-\alpha_-(\xi_2 + \alpha_+ \Xi(\epsilon) - (\alpha_+ - \alpha_-) \xi_1)} = K_1 e^{-\frac{\alpha_- K_2}{\epsilon}},$$

where $K, 1$ and K_2 are positive constants. We therefore have that as $\epsilon \rightarrow 0$ then $a(\Xi(\epsilon)) \rightarrow 0$, as well.

For b , the result is more immediate, as we have

$$|b(\xi)| \leq |b(\xi_1)| e^{\beta_+(\xi - \xi_1)} \leq \Delta e^{\beta_+(\xi - \xi_1)}.$$

This implies that

$$|b(\Xi(\epsilon))| \leq \Delta e^{\beta_+(\Xi(\epsilon) - \xi_1)},$$

and by hypothesis on $\Xi(\epsilon)$ we find that this also goes to zero in the limit as $\epsilon \rightarrow 0$. The solution to the slow component may be written in the implicit form

$$y(\Xi(\epsilon), \epsilon) = y_1(\xi_1, \epsilon) + \epsilon \int_{\xi_1}^{\Xi(\epsilon)} g(a(\sigma, \epsilon), b(\sigma, \epsilon), y(\sigma, \epsilon), \epsilon) d\sigma.$$

Since the box D is compact, we may take the supremum over D and arrive at

$$\|y(\Xi(\epsilon), \epsilon) - y_1(\xi_1, \epsilon)\| \leq \epsilon(\Xi(\epsilon) - \xi_1)L.$$

By the hypothesis on $\Xi(\epsilon)$ and y_1 , we arrive at the desired result. Since the convergence to zero of a and b is exponential, we find that the second part of the result follows, as well. ■

B.2 Corner estimates - the flow near the knee

At non-hyperbolic points, a Fenichel normal form does not exist, and therefore the techniques in Lemma 5 do not apply directly. Instead, we will use the normal form for a fold point derived in [23] to divide the domain into three pieces: one where the solution evolves at an $\mathcal{O}(\epsilon)$ rate, a second where the solution is pointwise $\mathcal{O}(\epsilon^{1/3})$ close to the non-hyperbolic knee, and a third where the solution is pointwise $\mathcal{O}(\epsilon^{1/3})$ close to the singular solution along the back. In fact, this decomposition has already been done in [23] in terms of various coordinate charts, so our task will be to confirm that their decomposition satisfies the properties that we are interested in.

We recall from the existence proof the normal form for a fold point presented in [23],

$$\begin{aligned} x' &= -y + x^2 + \mathcal{O}(\epsilon, xy, y^2, x^3) \\ y' &= -\epsilon + \mathcal{O}(\epsilon x, \epsilon y, \epsilon^2) \\ \epsilon' &= 0. \end{aligned} \tag{B.1}$$

This system was analyzed using geometric desingularization techniques. The approach is to introduce a change of coordinates,

$$x = \bar{r}\bar{x}, \quad y = \bar{r}^2\bar{y}, \quad \epsilon = \bar{r}^3\bar{\epsilon},$$

where $\bar{x}^2 + \bar{y}^2 + \bar{\epsilon}^2 = 1$. In this way, the degenerate point at the origin is blown-up to a sphere. Instead of analyzing the system in these coordinates, it is convenient to work in various coordinate charts. The three charts K_1, K_2 and K_3 are introduced in [23] and are described using the local coordinates

$$\begin{aligned} x &= r_1 x_1, & y &= r_1^2, & \epsilon &= r_1^3 \epsilon_1, \\ x &= r_2 x_2, & y &= r_2^2 y_2, & \epsilon &= r_2^3, \\ x &= r_3, & y &= r_3^2 y_3, & \epsilon &= r_3^3 \epsilon_3. \end{aligned}$$

Recall the definition of the entry and exit subsections for some value of $\rho > 0$,

$$\begin{aligned} \Delta^{in} &= \{(x, \rho^2), x \in J\} \\ \Delta^{out} &= \{(\rho, y), y \in \mathbb{R}\}, \end{aligned}$$

Definition 3. For $\rho > 0$ and $\delta > 0$, both small but $\mathcal{O}(1)$ with respect to ϵ , we define entry and exit subsections for the the charts defined above.

$$\begin{aligned} \Sigma_1^{in} &:= \{(x_1, r_1, \epsilon_1) | x_1 \in \mathbb{R}, r_1 = \rho, \epsilon_1 \in [0, \delta]\} \\ \Sigma_1^{out} &:= \{(x_1, r_1, \epsilon_1) | x_1 \in \mathbb{R}, r_1 \in [0, \rho], \epsilon_1 = \delta\} \\ \Sigma_2^{in} &:= \{(x_2, y_2, r_2) | y_2 = \delta^{-2/3}\} \\ \Sigma_2^{out} &:= \{(x_2, y_2, r_2) | x_2 = \delta^{-1/3}\} \\ \Sigma_3^{in} &:= \{(r_3, y_3, \epsilon_3) | r_3 \in [0, \rho], y_3 \in [-\beta_3, \beta_3], \epsilon_3 = \delta\} \\ \Sigma_3^{out} &:= \{(r_3, y_3, \epsilon_3) | r_3 = \rho, y_3 \in [-\beta_3, \beta_3], \epsilon_3 \in [0, \delta]\}. \end{aligned}$$

The flow from the entry subsection Δ^{in} to Δ^{out} is described with the aid of transition maps $\Pi_1 : \Sigma_1^{in} \rightarrow \Sigma_1^{out}$, $\Pi_2 : \Sigma_2^{in} \rightarrow \Sigma_2^{out}$ and $\Pi_3 : \Sigma_3^{in} \rightarrow \Sigma_3^{out}$.

The following facts are shown in [23].

Theorem 6. [23] There exists constants $\rho > 0$ and $\delta > 0$, both $\mathcal{O}(1)$ for which the trajectory entering Δ^{in} , exponentially close to the slow manifold has the following properties:

1. The derivative of any trajectory that stays $\mathcal{O}(\epsilon)$ close to the slow manifold in chart K_1 has a derivative bounded by $\mathcal{O}(\epsilon)$
2. While in chart K_2 , the tracked trajectory is $\mathcal{O}(\epsilon^{1/3})$ close to the fold point.
3. While in chart K_3 , the tracked slow manifold is $\mathcal{O}(\epsilon^{1/3})$ pointwise close in χ to the flow for the reduced ($\epsilon = 0$) system along the back

The proofs of 1 and 2 follow from [23]. We will establish 3 in the following lemma.

Lemma B.1. *Consider the fold-point normal form (B.1). There exists a function $\Xi(\epsilon)$ such that if $x(0, \epsilon) = \rho$, $y(0, \epsilon) = \mathcal{O}(\epsilon^{2/3})$ then there exist a $K > 0$ for which*

$$|(x, y)(t, \epsilon) - (x(t), 0)| < K\epsilon^{1/3}$$

Proof: We desingularize as in [23]. Let $x = \sigma$, $y = \sigma^2 y_3$, and $\epsilon = \sigma^3 \epsilon_3$. Then equation (B.1) is transformed to

$$\begin{aligned}\sigma' &= \sigma^2 F(\sigma, y_3, \epsilon_3) \\ y_3' &= \epsilon_3 \sigma (-1 + \mathcal{O}(\sigma)) - 2y_3 \sigma F(\sigma, y_3, \epsilon_3) \\ \epsilon_3' &= -3\epsilon_3 \sigma F(\sigma, y_3, \epsilon_3),\end{aligned}\tag{B.2}$$

where $F = 1 - y_3 + \mathcal{O}(\sigma)$. We consider initial conditions of the form,

$$x(0) = \rho, \quad y(0) = \kappa \epsilon^{2/3},$$

which transform to the initial conditions,

$$\sigma(0) = \rho, \quad y_3(0) = \kappa \frac{\epsilon^{2/3}}{\rho^2}, \quad \epsilon_3(0) = \frac{\epsilon}{\rho^3}.$$

The vector field in (B.2) may be desingularized by defining a new time scale,

$$\tau = \int_0^t \sigma(s) F(\sigma(s), y_3(s), \epsilon_3(s)) ds.\tag{B.3}$$

Provided that $F \neq 0$, this rescaling of the independent variable serves only to change the time parametrization of solutions. In the new variables, we have

$$\begin{aligned}\dot{\sigma} &= \sigma \\ \dot{y}_3 &= -2y_3 - \frac{\epsilon_3}{1 - y_3} + \sigma \epsilon_3 G(\sigma, y_3, \epsilon_3) \\ \dot{\epsilon}_3 &= -3\epsilon_3.\end{aligned}$$

The nonlinear term $\frac{\epsilon_3}{1 - y_3}$ is non-resonant and can therefore be transformed away using a smooth change of coordinates. This system is (in new coordinate \tilde{y}_3) is

$$\begin{aligned}\dot{\sigma} &= \sigma \\ \dot{\tilde{y}}_3 &= -2\tilde{y}_3 - \epsilon_3 + \sigma \epsilon_3 H(\sigma, \tilde{y}_3, \epsilon_3) \\ \dot{\epsilon}_3 &= -3\epsilon_3.\end{aligned}$$

This system may be solved implicitly as

$$\begin{aligned}\sigma(\tau) &= e^\tau \sigma(0) \\ \tilde{y}_3(\tau) &= e^{-2\tau} \tilde{y}_3(0) + \epsilon_3(0) e^{-2\tau} (e^{-\tau} - 1) + \sigma(0) \epsilon_3(0) e^{-2\tau} \int_0^\tau H(\sigma(s), \tilde{y}_3(s), \epsilon_3(s)) ds \\ \epsilon_3(\tau) &= e^{-3\tau} \epsilon_3(0).\end{aligned}\tag{B.4}$$

A contraction mapping argument and the fact that H is at least C^1 in y_3 shows that there exists a unique y_3 solving (B.4) so long as $(\sigma, y_3, \epsilon_3)$ stays in the compact set

$$D := \{(\sigma, y_3, \epsilon_3) | \sigma \in [0, \rho], y_3 \in [-\beta_3, \beta_3], \epsilon_3 \in [0, \delta]\}.$$

Noting the initial conditions, we see that the solution is defined on the interval $(\tilde{\Xi}, 0)$ with $\tilde{\Xi} = \frac{1}{3} \log(\frac{\epsilon_3(0)}{\delta})$.

$$\begin{aligned}\sigma(\tilde{\Xi}) &= \delta^{-1/3} \epsilon_3(0)^{1/3} \sigma(0) \\ \tilde{y}_3(\tilde{\Xi}) &= \frac{\tilde{y}_3(0) \delta^{2/3}}{\epsilon_3(0)^{2/3}} + \delta - \epsilon(0)^{1/3} \delta^{2/3} - \sigma(0) \epsilon_3(0)^{1/3} \delta^{2/3} \int_0^{\tilde{\Xi}} H(\sigma(s), \tilde{y}_3(s), \epsilon_3(s)) ds \\ \epsilon_3(\tilde{\Xi}) &= \delta.\end{aligned}$$

Note first that $(\sigma(\tilde{\Xi}), y_3(\tilde{\Xi}), \epsilon_3(\tilde{\Xi})) \in \Sigma_3^{in}$. Also, we have $\sigma(0) = \rho$, $y_3(0) = \kappa \frac{\epsilon^{2/3}}{\rho^2}$ and $\epsilon_3(0) = \frac{\epsilon}{\rho^3}$. Reverting to original variables we have,

$$\begin{aligned}x(\tilde{\Xi}) &= \delta^{-1/3} \epsilon^{1/3} \\ y(\tilde{\Xi}) &= \mathcal{O}(\epsilon^{2/3}) \\ \epsilon(\tilde{\Xi}) &= \epsilon,\end{aligned}$$

with $\tilde{\Xi} = \frac{1}{3} \log(\frac{\epsilon}{\delta \rho^3})$. This gives the transition time between Σ_3^{in} and Σ_3^{out} in terms of the τ timescale. Let Ξ be the transition time in the t timescale. Then (B.3) provides,

$$\tilde{\Xi} = \int_0^{\Xi} \sigma(\sigma) F(\sigma(s), y_3(s), \epsilon_3(s)) ds.$$

To compute the leading order description of Ξ , we note that $\sigma(s) = \mathcal{O}(-1/s)$ as $s \rightarrow -\infty$. Using the fact that $F = 1 - y_3 + \mathcal{O}(\sigma)$, we derive

$$\tilde{\Xi} \sim - \int_{\Xi}^{\mathcal{O}(1)} \frac{-C}{s} ds.$$

This implies that

$$\Xi \sim -C e^{-\tilde{\Xi}} \sim \mathcal{O}(\epsilon^{-1/3}).$$

An easy computation shows that this solution remains pointwise close to the $\epsilon = 0$, $y = 0$ solution on the interval $(\tilde{\Xi}, 0)$. ■

C Brief review of roughness of dichotomy results

The existence of the exponential dichotomies on each subinterval will follow from various roughness of dichotomy results. For completeness we list those results here.

Theorem 7. (Proposition 4.1 in [6]) *Let $x \in \mathbb{R}^n$ and suppose that the linear system $x' = A(\xi)x$ has an exponential dichotomy on J . Then, the linear system $x' = (A(\xi) + B(\xi))x$ also has an exponential dichotomy on J provided that $|B(\xi)| < \delta$ for all $\xi \in J$, for some δ sufficiently small.*

Note that the decay rates of the exponential dichotomy will be altered by $\mathcal{O}(\delta)$ amounts. A stronger result is provided by the following theorem.

Theorem 8. (Chapter 4 of [7]) *Suppose that $x' = Ax$ has an exponential dichotomy on J . Suppose that*

$$\int_J |B(\xi)| d\xi < \infty,$$

then the system $x' = (A + B(\xi))x$ also has an exponential dichotomy on J with the same decay rates as the original exponential dichotomy.

A final result will be useful for the analysis along the slow manifolds.

Theorem 9. (Proposition 6.1 in [6]) *Suppose that the $n \times n$ matrix $A(\xi)$ is bounded and hyperbolic for all $\xi \in J$ with k eigenvalues with real part less than $-\alpha < 0$ and $n - k$ eigenvalues with real part greater than $\beta > 0$. In addition, suppose that $A(\xi)$ is continuously differentiable and there exists a $\delta > 0$ such that $|A'(\xi)| < \delta$ for all $\xi \in J$. Then the linear system $x' = A(\xi)x$ has an exponential dichotomy on J .*

References

- [1] R. R. Aliev and A. V. Panfilov. A simple two-variable model of cardiac excitation. *Chaos, Solitons & Fractals*, 7(3):293 – 301, 1996.
- [2] P. W. Bates and C. K. R. T. Jones. Invariant manifolds for semilinear partial differential equations. In *Dynamics reported, Vol. 2*, volume 2 of *Dynam. Report. Ser. Dynam. Systems Appl.*, pages 1–38. Wiley, Chichester, 1989.
- [3] M. Beck, C. K. R. T. Jones, D. Schaeffer, and M. Wechselberger. Electrical waves in a one-dimensional model of cardiac tissue. *SIAM J. Appl. Dyn. Syst.*, 7(4):1558–1581, 2008.
- [4] G. A. Carpenter. A geometric approach to singular perturbation problems with applications to nerve impulse equations. *J. Differential Equations*, 23(3):335–367, 1977.
- [5] R. G. Casten, H. Cohen, and P. A. Lagerstrom. Perturbation analysis of an approximation to the Hodgkin-Huxley theory. *Quart. Appl. Math.*, 32:365–402, 1974/75.
- [6] W. Coppel. Dichotomies in stability theory. *Lecture Notes in Mathematics*, 629:1–98, 1978.
- [7] W. A. Coppel. *Stability and asymptotic behavior of differential equations*. D. C. Heath and Co., Boston, Mass., 1965.
- [8] F. Dumortier. Techniques in the theory of local bifurcations: blow-up, normal forms, nilpotent bifurcations, singular perturbations. In *Bifurcations and periodic orbits of vector fields (Montreal, PQ, 1992)*, volume 408 of *NATO Adv. Sci. Inst. Ser. C Math. Phys. Sci.*, pages 19–73. Kluwer Acad. Publ., Dordrecht, 1993.
- [9] E. Eszter. *Evans function analysis of the stability of periodic travelling wave solutions associated with the Fitzhugh-Nagumo system*. PhD thesis, University of Massachusetts, Amherst, 1999.
- [10] J. W. Evans. Nerve axon equations. IV. The stable and the unstable impulse. *Indiana Univ. Math. J.*, 24(12):1169–1190, 1974/75.
- [11] N. Fenichel. Persistence and smoothness of invariant manifolds for flows. *Indiana Univ. Math. J.*, 21:193–226, 1971/1972.
- [12] P. C. Fife and J. B. McLeod. The approach of solutions of nonlinear diffusion equations to travelling front solutions. *Arch. Ration. Mech. Anal.*, 65(4):335–361, 1977.
- [13] R. A. Gardner and C. K. R. T. Jones. Stability of travelling wave solutions of diffusive predator-prey systems. *Trans. Amer. Math. Soc.*, 327:465–524, 1991.
- [14] A. Ghazaryan, Y. Latushkin, and S. Schechter. Stability of traveling waves for degenerate systems of reaction diffusion equations. *Indiana Univ. Math. J.*, 60:443–472, 2011.
- [15] S. P. Hastings. On the existence of homoclinic and periodic orbits for the Fitzhugh-Nagumo equations. *Quart. J. Math. Oxford Ser. (2)*, 27(105):123–134, 1976.
- [16] G. A. Holzapfel. *Nonlinear Solid Mechanics : A Continuum Approach for Engineering*. Chichester, Inglaterra : Wiley, 2000.
- [17] C. K. R. T. Jones. Stability of the travelling wave solution of the FitzHugh-Nagumo system. *Trans. Amer. Math. Soc.*, 286(2):431–469, 1984.
- [18] C. K. R. T. Jones. Geometric singular perturbation theory. In *Dynamical systems (Montecatini Terme, 1994)*, volume 1609 of *Lecture Notes in Math.*, pages 44–118. Springer, Berlin, 1995.
- [19] C. K. R. T. Jones and N. Kopell. Tracking invariant manifolds with differential forms in singularly perturbed systems. *J. Differential Equations*, 108(1):64–88, 1994.

- [20] J. Keener and J. Sneyd. *Mathematical physiology*, volume 8 of *Interdisciplinary Applied Mathematics*. Springer-Verlag, New York, 1998.
- [21] P. Kohl, P. Hunter, and D. Noble. Stretch-induced changes in heart rate and rhythm: clinical observations, experiments and mathematical models. *Progress in Biophysics and Molecular Biology*, 71(1):91 – 138, 1999.
- [22] A. Kolmogorov, I. Petrovskii, and N. Piscounov. Etude de l’équation de la diffusion avec croissance de la quantité de matière et son application à un problème biologique. *Moscow Univ. Math. Bull.*, 1:1–25, 1937.
- [23] M. Krupa and P. Szmolyan. Extending geometric singular perturbation theory to nonhyperbolic points—fold and canard points in two dimensions. *SIAM J. Math. Anal.*, 33(2):286–314, 2001.
- [24] N. H. L. Kuijpers, H. M. M. ten Eikelder, P. H. M. Bovendeerd, S. Verheule, T. Arts, and P. A. J. Hilbers. Mechanoelectric feedback leads to conduction slowing and block in acutely dilated atria: a modeling study of cardiac electromechanics. *Am J Physiol Heart Circ Physiol*, 292(6):H2832–2853, 2007.
- [25] L. Malvern. *Introduction to the mechanics of a continuous medium*. Prentice Hall, Englewood Cliffs, 1986.
- [26] H. P. McKean, Jr. Nagumo’s equation. *Advances in Math.*, 4:209–223 (1970), 1970.
- [27] M. P. Nash and A. V. Panfilov. Electromechanical model of excitable tissue to study reentrant cardiac arrhythmias. *Progress in Biophysics and Molecular Biology*, 85(2-3):501 – 522, 2004. Modelling Cellular and Tissue Function.
- [28] K. Palmer. Exponential dichotomies and transversal homoclinic points. *JDE*, 55:225–256, 1984.
- [29] K. Palmer. Exponential dichotomies and fredholm operators. *Proc. AMS*, 104:149–156, 1988.
- [30] A. V. Panfilov, R. H. Keldermann, and M. P. Nash. Self-organized pacemakers in a coupled reaction-diffusion-mechanics system. *Phys. Rev. Lett.*, 95(25):258104, Dec 2005.
- [31] D. Peterhof, B. Sandstede, and A. Scheel. Exponential dichotomies for solitary-wave solutions of semi-linear elliptic equations on infinite cylinders. *J. Differential Equations*, 140(2):266–308, 1997.
- [32] J. Rinzel and J. B. Keller. Traveling wave solutions of a nerve conduction equation. *Biophysical Journal*, 13(12):1313 – 1337, 1973.
- [33] J. Rottmann-Matthes. Linear stability of traveling waves in first-order hyperbolic pdes. *Journal of Dynamics and Differential Equations*, 23:365–393, 2011. 10.1007/s10884-011-9216-3.
- [34] B. Sandstede. Stability of travelling waves. In *Handbook of dynamical systems, Vol. 2*, pages 983–1055. North-Holland, Amsterdam, 2002.
- [35] J. Smoller. *Shock waves and reaction-diffusion equations*, volume 258 of *Grundlehren der Mathematischen Wissenschaften [Fundamental Principles of Mathematical Science]*. Springer-Verlag, New York, 1983.
- [36] A. I. Volpert, V. A. Volpert, and V. A. Volpert. *Traveling wave solutions of parabolic systems*, volume 140 of *Translations of Mathematical Monographs*. American Mathematical Society, Providence, RI, 1994. Translated from the Russian manuscript by James F. Heyda.
- [37] Y. Wu, X. Xing, and Q. Ye. Stability of travelling waves with algebraic decay for n -degree Fisher-type equations. *Discrete Contin. Dyn. Syst.*, 16(1):47–66, 2006.
- [38] J. Xin. Front propagation in heterogeneous media. *SIAM Rev.*, 42(2):161–230, 2000.
- [39] R. Yoshida, T. Takahashi, T. Yamaguchi, and H. Ichijo. Self-oscillating gel. *Journal of the American Chemical Society*, 118(21):5134–5135, 1996.